Extending the Scope of Conceptual Density Functional Theory with Second Order Analytical Methodologies

Wang, Bin; Geerlings, Paul; Liu, Shubin; De Proft, Frank

Published in:
Journal of Chemical Theory and Computation

DOI:
10.1021/acs.jctc.3c01184

Publication date:
2024

License:
Unspecified

Document Version:
Accepted author manuscript

Extending the Scope of Conceptual DFT with Second Order Analytical Methodologies

Bin Wang[1], Paul Geerlings[1], Shubin Liu[2,3], Frank De Proft[1*]

[1] *Research Group of General Chemistry (ALGC), Vrije Universiteit Brussel (VUB), Pleinlaan 2, B-1050 Brussels, Belgium. E-mail:* fdeprof@vub.be

[2]*Research Computing Center, University of North Carolina, Chapel Hill, North Carolina 27599-3420, United States*

[3]*Department of Chemistry, University of North Carolina, Chapel Hill, North Carolina 27599-3290, United States*

Author	**ORCID Numbers**
BW	0000-0003-3611-5451
PG	0000-0003-1897-7285
SL	0000-0001-9331-0427
FDP	0000-0003-4900-7513

ABSTRACT

In the context of the growing impact of conceptual density functional theory as one of the most successful chemical reactivity theories, response functions up to second order have now been widely applied; in recent years, among others, particular attention has been focused on the linear response function and also extensions to higher order have been put forward. As the larger part of these studies have been carried using a finite difference approach to compute these concepts, we now embarked in (an extension of) an analytical approach to conceptual DFT. With the ultimate aim of providing a complete set of analytically computable second order properties, including the softness and hardness kernels, the hardness as the simplest second order response function is scrutinized again with numerical results highlighting the difference in nature between the analytical hardness (referred as hardness condition) and the Parr-Pearson absolute chemical hardness. The hardness condition is investigated on its the capability to gauge the (de)localization error of DFAs. The analytical Fukui function, besides overcoming the difficulties in the finite difference approach in treating negatively charged systems, also showcases the errors of deviating from the straight-line behavior using fractional occupation number calculations. Subsequently, the softness kernel and its atom-condensed inverse, the hardness matrix, are accessed through the Berkowitz-Parr relation. Revisiting the softness kernel confirms and extends previous discussions on how Kohn's Nearsightedness of Electronic Matter principle can be retrieved and identified as the physicist's version of the chemist's "transferability of functional groups" concept. The accurate, analytical hardness matrix evaluation on the other hand provides further support for the basics of Nalewajski's charge sensitivity analysis. Based on Parr and Liu's functional expansion of the energy functional, a new energy decomposition is introduced with an order of magnitude analysis of the different terms for a series of simple molecules both at their equilibrium geometry and upon variation in bond length and dihedral angle. Finally, for the first time, the perturbation expansion of the energy functional is studied numerically up to second order now that all response functions and integration techniques are at

hand. The perturbation expansion energies are in excellent agreement with those obtained directly from DFA calculations giving confidence in the convergence of the perturbation series and its use in judging the importance of the different terms in reactivity investigations.

1. Introduction

Since the growing development of conceptual density functional theory (CDFT),[1-9] also often referred to as density functional reactivity theory (DFRT),[7] the theory has gained worldwide attention as a firmly rooted chemical reaction theory. Launched by Parr et al in the late 1970s,[1, 10, 11] CDFT has been instrumental in providing sharp definitions for a number of often well-known but often vaguely defined concepts such as electronegativity,[10, 12] hardness…[13, 14] enabling, in principle, their numerical evaluation. The central role in this endeavor and adopting the most frequently used canonical ensemble (vide infra) is played by a series of response functions of the type $(\delta^n E/\partial N^m \delta v(\boldsymbol{r_1})\delta v(\boldsymbol{r_2}) \ldots \delta v(\boldsymbol{r_{m'}}))$,[15, 16] with $n = m + m'$, reflecting the sensitivity of the system's energy to variations in the number of electrons and/or the external potential. Whereas in the early years of CDFT, most attention was devoted to the first order derivatives (the electronic chemical potential[10] μ and the density $\rho(\boldsymbol{r})$ itself), and two of the second order derivatives, hardness[13] $[\partial^2 E/\partial^2 N]_v$ and the Fukui function[17, 18] $\delta^2 E/\partial N \delta v(\boldsymbol{r}) = [\delta\rho(\boldsymbol{r})/\partial N]_v$, the scope was later extended to some of the third order derivatives, especially the dual descriptor[19, 20] $[\delta f(\boldsymbol{r})/\partial N]_v$, and gradually also to the "third" second order derivative, the so-called linear response function $[\delta^2 E/\delta v(\boldsymbol{r})\delta v(\boldsymbol{r}')]_N$, usually denoted as $\chi(\boldsymbol{r}, \boldsymbol{r}')$.[11, 21, 22] Although well known in its time or frequency dependent form in time-dependent DFT[23-26] through the Casida equations,[27, 28] the time-independent form received relatively little attention due to computational intricacies, the representation of this kernel and an adequate chemical interpretation of the results. Parallel progress was made in these three issues. The independent particle approximation derived from a coupled perturbed HF or KS approach was refined to a full (exact) DFT expression using functionals from the first four rungs of Jacob's ladder of exchange-correlation functionals.[29] Different visualization strategies were developed from radial distribution type plots for atoms to molecular iso-surfaces.[29] The interpretational progress is largely based on the identity that $\chi(\boldsymbol{r}, \boldsymbol{r}')$ can be written as $[\delta\rho(\boldsymbol{r})/\delta v(\boldsymbol{r}')]_N$ showing that the LRF provides information on the variation of the electron density at position $\boldsymbol{r}$ when the external potential at position $\boldsymbol{r}'$ is changed,

obviously a key issue when evaluating chemical reactivity. This has led to retrieving atomic shell structure,[30-32] inductive and mesomeric effects,[33] aromaticity and anti-aromaticity,[34-36] electron delocalization,[37] up to deciphering its role in electrical conductivity[38] and formulating some initial results on reconciling the Nearsightedness of Electronic Matter principle put forward by Prodan and Kohn [39, 40] with the chemist's functional group concept.[41]

Having now the analytical expression of the linear response function $\chi(\boldsymbol{r},\boldsymbol{r}')$ and its numerical comparison study on possible approximations as well as on different density functionals at hand, it is natural to think one step further and pass to the counterpart of the linear response function in the grand canonical ensemble: the softness kernel $s(\boldsymbol{r},\boldsymbol{r}')$ defined as $s(\boldsymbol{r},\boldsymbol{r}') = [\delta^2\Omega/\delta v(\boldsymbol{r})\delta v(\boldsymbol{r}')]_\mu = [\delta\rho(\boldsymbol{r})/\delta v(\boldsymbol{r}')]_\mu$,[11, 42], with Ω being the so-called grand potential. Although already appearing and discussed in early literature by Parr and Yang and in their standard DFT treatise[11] the maybe most illuminating aspect of softness kernel emerged later on when Kohn and Prodan formulated their principle of nearsightedness of electronic matter (NEM).[39, 40] Starting from their definition of nearsightedness: "…describing the fact that, for fixed chemical potential μ, local electronic properties, such as the density $\rho(\boldsymbol{r})$, depend significantly on the effective external potential $v(\boldsymbol{r})$ only at nearby points" a close relationship with the softness kernel emerges. The basic ingredients are indeed identical: working at constant chemical potential and observing the variation of ρ with v ask for checking if $s(\boldsymbol{r},\boldsymbol{r}')$ decays quickly upon increasing distance between $\boldsymbol{r}$ and $\boldsymbol{r}'$. Since different ensembles are related by Legendre transformations, the softness kernel can be evaluated starting from the linear response function via the Berkowitz-Parr relation (vide infra).[42] Given the fact that this relation requires information not only for the linear response function but for also the Fukui function at $\boldsymbol{r}$ and $\boldsymbol{r}'$ and the hardness, in order to quantitatively achieve such relation, we would need to formulate analytical expressions for *all* the second order CDFT quantities in order to evaluate the softness kernel via the Berkowitz-Parr relation. Some initial work along these lines, with results pointing into the expected direction, has been presented by one of

the present authors,[41] the aim of the present study is however broader pertaining analytical evaluation and use of all second derivatives in different contexts.

In the present work, we first formulate the analytical expression for all CDFT descriptors up to the second order in the canonical ensemble in a uniform way, thereby completing previous expressions.[29, 43] Before going directly to the softness kernel, we first investigate in detail the behavior of the two others second order derivatives i.e., the hardness and Fukui function for which the use of an analytical expression was scrutinized in the literature only in a very limited number of cases.

We distinguish the physical significance of the chemical hardness as identified by Parr and Pearson and the hardness condition from CDFT[43] arising when evaluating analytically the second derivative of E w.r.t. N as a consequence of the piecewise linear behavior of the E vs N curve.[44] We demonstrate the application of this condition, which exact exchange-correlation functionals should obey, for the evaluation and design of these functionals. We then compare the results of analytical and finite difference methods for calculating the Fukui function, examining the robustness of the widely used finite difference approach in assessing electrophilicity and nucleophilicity and relate some discrepancies to delocalization errors.

Passing then to evaluation of the softness kernel the NEM principle is scrutinized in a homologous series of substituted alkenes and alkanes, completing the prior results in previous work mentioned above.[29, 41] The softness kernel availability then brings back to the forefront an older, actually less used reactivity indicator, which can easily be obtained once the softness kernel is available, namely the hardness kernel which is just its inverse.[11, 22, 45] Launched in the late 1980s by Nalewajski[46, 47] in a semi-empirical context of Mortier's electronegativity equalization method (EEM),[48] the eigenvalues and eigenvectors of the atom-condensed hardness matrix lead to a normal mode type analysis where the different population normal modes reflect charge transfer or polarization phenomena when a system's number of electrons changes. The availability of analytical softness matrices enables us to test the qualitative agreement for some selected cases with older literature data and further reflect on their physical content.

In the final section and with the availability of all first and second order CDFT quantities, we scrutinize in a numerical study, the first of its kind to the best of our knowledge, two expansions of the total energy. The context of the first one is the perturbation perspective usually adopted in CDFT following Parr's initial ansatz (response of a system's energy to perturbations in N and/or v) (vide supra).[1, 3, 11] The other one, launched by Liu and Parr which hitherto received less attention, is a functional expansion of E in terms of N and v.[49-51] In both cases numerical values for each term up to second order could now be evaluated enabling an order of magnitude analysis and an evaluation of the importance of the contributing terms. In the functional Taylor expansion, a new CDFT based way of decomposing the total- unperturbed- energy is thereby obtained. The choice of systems is made in such a way as to combine simplicity and relevance for the study of the different topics mentioned above.

The paper is structured as follows. Section 2, **Methodology**, gives all the formulas used for calculating the analytical CDFT descriptors as well as the ensemble transformations. **Computational Details** are provided in Section 3. In Section 4, **Results and Discussion**, results are addressed and presented in the five different subtopics mentioned above: hardness and hardness condition (4.1), Fukui function and delocalization error (4.2), softness kernel and nearsightedness revisited (4.3), hardness kernel and electron population modes (4.4) and perturbation expansion and energy decomposition (4.5). The capabilities of (analytical) second order CDFT and related extensions are thereby illustrated. Section 5, **Conclusion**, summarizes the results of the paper and explores the applicability and importance of analytical CDFT in future theoretical chemistry research.

2. Methodology

In the larger part of the literature the second order conceptual DFT quantities are obtained following either the finite difference (FD) or frontier orbital (FO) approximation. The chemical hardness is then written as[3, 11, 13]

$$\eta^{FD} = \frac{E_{N-1} - 2E_N + E_{N+1}}{2} \tag{1}$$

$$\eta^{FO} = \frac{\varepsilon_{LUMO} - \varepsilon_{HOMO}}{2} \tag{2}$$

which under certain conditions are identical.[52]

The Fukui function[17] is given by

$$f_{FD}^{-}(\boldsymbol{r}) = \rho_N(\boldsymbol{r}) - \rho_{N-1}(\boldsymbol{r}) \tag{3}$$

$$f_{FD}^{+}(\boldsymbol{r}) = \rho_{N+1}(\boldsymbol{r}) - \rho_N(\boldsymbol{r}) \tag{4}$$

$$f_{FO}^{-}(\boldsymbol{r}) = \rho_{HOMO}(\boldsymbol{r}) \tag{5}$$

$$f_{FO}^{+}(\boldsymbol{r}) = \rho_{LUMO}(\boldsymbol{r}) \tag{6}$$

Where the E_{N-1}, E_{N+1}, ρ_{N-1} and ρ_{N+1}represent the energy and electron density of the cationic and anionic system, the N electron system being considered to be neutral, and the HOMO/LUMO orbital energy and density are denoted as ε_{HOMO}, ε_{LUMO}, ρ_{HOMO} and ρ_{LUMO}.

Considering closed shell systems for computational simplicity compact analytical expressions for all these conceptual DFT quantities can be written. For example, the well-known expressions for the first order derivatives of the total energy $E[N, v(\boldsymbol{r})]$, the chemical potential μ also known as the frontier orbital energy ε_f, and the density $\rho(\boldsymbol{r})$ are[11, 43]

$$\left(\frac{\partial E}{\partial N}\right)_v = \mu = \langle \varphi_f | \hat{h}_{eff} | \varphi_f \rangle = \varepsilon_f \tag{7}$$

$$\left(\frac{\partial E}{\delta v(\boldsymbol{r})}\right)_N = \rho(\boldsymbol{r}) = \sum_{i=1}^{N} |\varphi_i(\boldsymbol{r})|^2 \tag{8}$$

Where $\hat{h}_{eff}$ is the effective one-electron Hamiltonian, and $\varphi_i(\boldsymbol{r})$ and ε_f are the molecular orbital and frontier orbital energies respectively. Using the coupled-perturbed Hartree-Fock (CPHF)[53] or Kohn-Sham[54] (CPKS) approach for the second order CDFT descriptors, the linear response function can be written as[43]

$$\left(\frac{\partial E}{\delta v(\boldsymbol{r})\delta v(\boldsymbol{r}')}\right)_N = \chi(\boldsymbol{r},\boldsymbol{r}') = -4\sum_{ia,jb}(\mathbb{M}^{-1})_{ia,jb}\varphi_i(\boldsymbol{r})\varphi_a(\boldsymbol{r})\,\varphi_j(\boldsymbol{r}')\varphi_b(\boldsymbol{r}') \tag{9}$$

where the $\mathbb{M}$ matrix for Kohn-Sham DFT is given by

$$\mathbb{M}_{ia,jb} = (\varepsilon_a - \varepsilon_i)\delta_{ij}\delta_{ab} + 4(ia|jb) + 4(ia|f_{xc}(\boldsymbol{r},\boldsymbol{r}')|jb) \tag{10}$$

Where we use indices i, j … for occupied and a, b … for virtual orbitals. The evaluation of the exchange-correlation kernel $f_{xc}(\boldsymbol{r},\boldsymbol{r}')$ and its integral for functionals including hybrid or other rungs in Jacob's ladder[55] can be found in **Ref. 43**. Different approximation schemes for the $\mathbb{M}$ matrix have been systematically investigated in our previous study.

Using a similar notation, the Fukui function can be written in a condensed way as

$$\frac{\partial E}{\partial N\delta v(\boldsymbol{r})} = f(\boldsymbol{r}) = \left|\varphi_f(\boldsymbol{r})\right|^2 - \sum_{ia,jb}(\mathbb{M}^{-1})_{ia,jb}\,\mathbb{K}^{ff}_{ff,ia}\varphi_j(\boldsymbol{r})\varphi_b(\boldsymbol{r}) \tag{11}$$

with the $\mathbb{K}^{ff}_{ia}$ matrix for Kohn-Sham DFT is defined as

$$\mathbb{K}^{ff}_{ff,ia} = 4(ff|ia) + 4(ff|f_{xc}(\boldsymbol{r},\boldsymbol{r}')|ia) \tag{12}$$

Similarly, the second derivative of E with respect to N, written in the case of closed shell Kohn-Sham DFT as

$$\left(\frac{\partial^2 E}{\partial N^2}\right)_v = \eta = \mathbb{K}^{eta}_{ff,ff} - \sum_{ia,jb}(\mathbb{M}^{-1})_{ia,jb}\,\mathbb{K}^{ff}_{ff,ia}\mathbb{K}^{eta}_{ff,jb} \tag{13}$$

with

$$\mathbb{K}^{eta}_{ff,ff} = (ff|ff) + (ff|f_{xc}(\boldsymbol{r},\boldsymbol{r}')|ff) \tag{14}$$

$$\mathbb{K}^{eta}_{ff,jb} = (ff|jb) + (ff|f_{xc}(\boldsymbol{r},\boldsymbol{r}')|jb) \tag{15}$$

Note that depending on the choice of the frontier orbital f (HOMO or LUMO) two quantities arise, corresponding to an electron release or electron uptake process with respect to the reference N value. In view of the piecewise linear behavior of the $E = E(N)$ curve both expressions become zero in the case of

the exact energy functional. This demand has been termed the "hardness condition" in previous work by Yang and the present authors.[43] Consequently, there are in fact two conditions depending on the choice of the frontier orbital.

A word of caution should therefore be introduced. Parr and Pearson's original identification of the chemical hardness[13] was based on a quadratic $E = E(N)$ curve thereby avoiding the derivative discontinuity problem arising from the piecewise linearity of this curve. Their identification, leading to the well-known finite difference **Eqn. 1** has gained widespread use and has been extremely useful in various domains of chemistry, thereby often bridging the theoretician's and experimentalist's worlds.[1-9] Its importance can hardly be overestimated. It is therefore not our aim to discard this venerable approach (see also **Ref. 8** for a recent discussion) but simply point out that, when adopting an internally consistent analytical approach, the expression corresponding with the second E vs. N derivative in fact boils down to the hardness conditions which, on themselves, deserve closer inspection as will be done in the present study.

Equations 10, 12, 14 and 15 can also be easily extend to other methods as Hartree-Fock and different DFA functionals (for a recent critical account see Teale et al)[56] varying from pure DFT functionals (LDA, GGA, meta GGA…) to hybrid and range-separated functionals (with modifications on the f_{xc} integral if exact exchange is also present).[29] However, in order to evaluate the hardness condition η for functionals including (part of) the exact exchange one needs to calculate the Fukui matrix[57] $f(\boldsymbol{r}, \boldsymbol{r}')$ which is the derivative of the one particle reduced density matrix $\rho(\boldsymbol{r}, \boldsymbol{r}')$ with respect to the number of electrons N.

$$f(\boldsymbol{r}, \boldsymbol{r}') = \frac{\delta\rho(\boldsymbol{r}, \boldsymbol{r}')}{\partial N} \tag{16}$$

which considerably complicates the computational aspects and will be the subject of a separate study. We therefore use, in the present study, only "pure" DFT functionals of the LDA, GGA and meta-GGA type.

To have access to the corresponding CDFT descriptors under the grand canonical ensemble characterized by the grand potential $\Omega = \Omega[\mu, v]$, related to the $E = E[N, v]$ functional via a Legendre transformation, the following expressions for the softness S and the local softness $s(\boldsymbol{r})$ are well-known[3, 11, 18]

$$S = \frac{1}{\eta} \tag{17}$$

$$s(\boldsymbol{r}) = S \cdot f(\boldsymbol{r}) \tag{18}$$

Finally, using the Berkowitz-Parr relation, the softness kernel $s(\boldsymbol{r}, \boldsymbol{r}')$, defined as $[-\delta^2\Omega/\delta v(\boldsymbol{r})\delta v(\boldsymbol{r}')]_N$ in the grand canonical ensemble, can be obtained from the three second order derivatives in the canonical ensemble

$$s(\boldsymbol{r}, \boldsymbol{r}') = \frac{f(\boldsymbol{r})f(\boldsymbol{r}')}{\eta} - \chi(\boldsymbol{r}, \boldsymbol{r}') \tag{19}$$

The hardness kernel $\eta(\boldsymbol{r}, \boldsymbol{r}')$ defined as $\delta^2 F/\delta\rho(\boldsymbol{r})\delta\rho(\boldsymbol{r}')$ [1, 22, 58]yields a reciprocity relation with the softness kernel in the sense that $\int s(\boldsymbol{r}, \boldsymbol{r}')\eta(\boldsymbol{r}, \boldsymbol{r}'')d\boldsymbol{r}' = \delta(\boldsymbol{r} - \boldsymbol{r}')$.

Introducing the atomic overlap matrix $S_{ij}^A = \int \varphi_i(\boldsymbol{r})\varphi_j(\boldsymbol{r})w^A(\boldsymbol{r})d\boldsymbol{r}$ for the atoms-in-molecules condensation we then arrive at the atom-condensed versions of the linear response function,

$$\chi_{AB} = -4\sum_{ia,jb}(\mathbb{M}^{-1})_{ia,jb}S_{ia}^A S_{jb}^B \tag{20}$$

the Fukui function,

$$f_A = S_{ff}^A - \sum_{ia,jb}(\mathbb{M}^{-1})_{ia,jb}\,\mathbb{K}_{ff,ia}^{ff}S_{jb}^A \tag{21}$$

and the softness kernel

$$s_{AB} = \frac{f_A f_B}{\eta} - \chi_{AB} \tag{22}$$

Thereby introducing the softness matrix $\boldsymbol{s}$ with the hardness matrix $\boldsymbol{\eta}$ being its inverse $\boldsymbol{s} = \boldsymbol{\eta}^{-1}$.

3. Computational Details

All geometry optimizations were performed at the B3LYP/cc-pVTZ level of theory[59-62] with tight convergence cutoffs using the Gaussian 16 A03 package.[63] Subsequent single point DFA (density functional approximation) calculations were carried out at the PBE/cc-pVTZ level of theory[64] using the PySCF 2.1.1 package.[65, 66] Point group symmetry was turned on for all single point calculations as will be explained in the context below. NWChem 7.0.2[67] was employed to perform DFA calculations with fractional occupation number and the 3.8 development version of Multiwfn[68] was then used to perform density and charge analysis. A Python program was built to compute all conceptual DFT quantities up to the softness kernel and the hardness kernel diagonalization following the single point PySCF calculations. Libxc 5.2.3[69] was employed to calculate the exchange-correlation kernel $f_{xc}(\boldsymbol{r}, \boldsymbol{r}')$. The Becke-Lebedev quadrature was used for numerical integration using grids with 99 radial and 590 angular points.[70] If not specified explicitly the evaluation of the exchange-correlation kernel is set to be the "full" expression i.e., for PBE functional we calculated the $f_{xc}(\boldsymbol{r}, \boldsymbol{r}')$ up to GGA expansion, as described in **Ref. 29**. The standard Hirshfeld approach was chosen for the atom-in-molecules (AIM) partitioning.[71-73] All units used in this paper, if not specified, are atomic units.

4. Results and Discussion

4.1 Chemical hardness and hardness condition

The starting equation in conceptual DFT is the energy functional written as a function of the number of electrons. It is piecewise linear from $N-1$ to N and N to $N+1$, and so on, as displayed in **Scheme 1a.** So, it is natural to have double-sided derivatives for instance as $\mu^{\pm}$, $\eta^{\pm}$ but also $f^{\pm}$, as the Fukui function can also (cf. Introduction) be written as $[\delta\mu/\delta v(\boldsymbol{r})]_N$.[11, 74] As the first order derivative of E with respect to N, μ, gives a step function the second order derivative η should be zero on both sides which is the hardness condition. As a result, all response properties including second or higher order derivative of N will in fact become zero for non-integer number of electrons $N \pm \lambda$ for the exact functional at 0K and are ill defined at integer values N, as illustrated in **Scheme 1b**. Again (vide supra) it is seen that the hardness calculated from **Eqn. 13** is not the Parr-Pearson chemical hardness but the hardness condition. So, what is the real, chemical hardness of the system in view of the venerable Parr-Pearson expression and the concomitant maximum hardness principle (MHP)?[3, 8, 75, 76]

As Yang et al. pointed out a simple way out is to use the fundamental gap, defined as $I-A$ or, equivalently, the HOMO-LUMO gap as the hardness[52] which aligns with **Eqn. 1 and 2.** Employing the $I-A$ value (resulting from a quadratic $E=E(N)$ curve) or the HOMO-LUMO gap is a sounder and chemically more meaningful candidate for chemical hardness than the hardness condition $\eta^{\pm}$. The same strategy can also be used to obtain higher order N-derivatives for example the hyper hardness $\gamma=[\partial^3 E/\partial N^3]_v$ yielding $\gamma=\varepsilon_{LUMO}-2\varepsilon_{HOMO}+\varepsilon_{HOMO-1}$, or mixed second order N-derivatives such as the dual descriptor. **Equation 13** on the other hand allows for a (far from unique) measure to estimate how much DFAs might differ from the exact functional as will be discussed quantitatively below. Along this line, the "sign problem" of chemical hardness can be simply resolved by setting $2\eta^{-}=2\eta^{+}=\varepsilon_{LUMO}-\varepsilon_{HOMO}$, a well-known practical example of it in the literature being the two-parabola model proposed by Vela et al.[77] Another way of addressing the derivative discontinuity is to include temperature in the energy functional

$E[N, v(\boldsymbol{r}), T]$ and a lot of efforts in this field have been made by Ayers et al.[78] The E v.s. N curve is smoothened by a not necessarily small temperature perturbation making it differentiable at the point N. In such way all response quantities are physically meaningful in theory but need to account for the temperature to which the system is exposed.

To quantify things, we report in **Table 1** the chemical potential $\mu^{\pm}$ (**Eqn. 7)**, the hardness η (**Eqn. 2**) and hardness conditions $\eta^{\pm}$ (**Eqn. 13)** for a set of di- and polyatomic systems. In accordance with the Parr-Pearson identification the hardness represents the resistance of a species to change its number of electrons and through the maximum hardness principle, although to be used with caution, it indicates the relative stability of the system. The value for hardness condition determines the deviation from the exact condition (its value being zero) and allows to judge the extent to which the DFA (like LDAs and GGAs etc.) are affected by delocalization errors, originating from the self-interaction error (SIE).[52, 79, 80] Therefore, the hardness condition can be used as criterion for evaluating the "quality" of the different density functional approximations. As can be seen from the table, the values of the HOMO hardness condition η^{-} at PBE/cc-pVTZ level of the theory are always positive and amount to about 0.3 to 0.4 a.u. with different trends for varying series of compounds, which lend themselves not to a direct interpretation as moreover, here, a single functional was used in this proof-of-concept part. This order of magnitude is important and can be compared with the typical value for the chemical hardness which rarely amounts to 0.5 a.u. The lack of correlation between the hardness condition and the chemical hardness with a correlation coefficient $R^2 < 0.3$ shows the fundamental difference between these two quantities, **Fig. S1**. The LUMO hardness condition η^{+} shows relatively similar results as η^{-},however, it gives negative values for the ionic systems. Deepening the content of **Scheme 1a** we now focus on the convex and concave features of most DFAs and the Hartree-Fock method showing a piecewise concave nature in the Hartree Fock case and in most DFAs a piecewise convex nature e.g., discussed in **Refs. 80 and 81** respectively.[80, 81] The overall positive values for the hardness condition are in line with a piecewise convex behavior, which is usually attributed to a

delocalization error yielding lower (relative) energies than it should be. On the other hand, the very few negative condition values (ionic systems on the electron abundant side) imply a concave behavior which indicates electrons are "too localized" for PBE in these few cases. To further use the hardness condition in evaluating density functionals, a first test in **Table 2** exhibits the total atomization energy $\sum D_e$ (TAE) and the two hardness conditions calculated for 19 commonly used pure density functionals including 2 LDA and 17 GGA functionals for water.[82] Although by going from LDA to GGA more accurate TAE values for water are obtained when comparing with the experimental result 0.371, hinting at increasing quality, energy-wise, the hardness conditions are not reduced significantly but rather show an increase of η^+ for some functionals illustrating that probably a test based on energy values evaluated only at integer N may not be an adequate test. This observation is in line with the results by Hait and Head-Gordon[80] in investigating the nature of (de)localization error in the basis of energy evaluations at fractional number of electrons thereby mimicking the nature of the full $E = E(N)$ curve. A study of the energy of fractionally ionized H_2O for a wide variety of functionals yielded quadratic curvature coefficients a (**Ref. 80 Fig. 6**), where the higher the a value in their work means the larger the hardness condition $\eta^{\pm}$ in our work. Among our selected functionals, the PBE family in **Table 2** behaves better than LYP, and among all of them the "best" well-behaved functional is PW91 which has both relatively small η^- and η^+ compared to others. Finally concentrating on the expression for the hardness condition, **Eqn. 13** shows that it is the difference between two terms, the first one involving two integrals comprising only the frontier orbital considered and the second one, resulting from a matrix multiplication with matrix elements involving all orbitals (occupied and unoccupied). For the exact functional with $\eta^{\pm} = 0$ they should precisely cancel each other. Also being noticed is the quadratic term matrix multiplication $\mathbf{K_{ia}^T M_{ia,jb} K_{jb}}$ appearing in the expression of the hardness condition which remarkably coincides with what Hait and head-Gordon have observed previously in investigating the quadratic behavior of the delocalization error in fractional occupation number.[80]

4.2 Fukui function and density delocalization error

Given the analytical expression of the Fukui function in **Eqn. 11 and 12,** the evaluation of the Fukui function needs the frontier orbital density $\left|\varphi_f(\boldsymbol{r})\right|^2$ and its two-electron integrals exhibited in the $\mathbb{K}_{ff,ia}^{ff}$ matrix. For non-degenerated systems the chosen frontier orbitals are unambiguously the HOMO and LUMO which then produce the two Fukui function f^- and f^+ as descriptors for nucleophilicity and electrophilicity respectively. For systems with HOMO or LUMO degeneracy the calculation of the analytical Fukui function needs to specify the frontier orbital(s) to be taken into account. For instance, as shown in **Scheme 1c**, for methane the HOMO is threefold degenerate whereas the LUMO is non-degenerate. Consequently, when evaluating f^- with a symmetry broken calculation the frontier orbital density and electron integrals will have different values due to spatial asymmetry though the three degenerate HOMOs will in the end have the same orbital energy. As a result, it turns out, as we indeed observed, that at each time the calculation is re-done, the arbitrary chosen HOMO is changed on each occasion with correspondingly varying final f^- values. For a simple and straightforward way of handling the degeneracy of frontier orbitals, we can either manually average the three degenerate HOMOs of a symmetry broken calculation or turn on the point group symmetry using symmetry adapted molecular orbitals to ensure that the molecular orbital coefficients are perfectly symmetric. Degenerated perturbation theory may, of course, be used but turns out to be computationally more demanding.[83] Therefore, throughout this work we always chose to turn on the point group symmetry constraint while performing single point calculations for the evaluation of Fukui functions as well as the hardness condition. **Table 1** shows the Fukui function for a set of di- and small polyatomic systems as reference data for forthcoming calculations and intermediate values for some of the present ones. Without going into detail previously discussed literature trends can be retrieved,[1-9] for example trends in the local softness values derived from these data. To compare properties between different system, we indeed have to shift from the Fukui function to the local softness $s^{\pm}(r) = S \cdot f^{\pm}(r) =$

$f^{\pm}(r)/\eta$,[1-3] where we have now used the Parr-Pearson chemical hardness. The local softness of the halogen atom decreases from HBr, HCl to HF with values 7.66, 6.46, 4.55 for s^- and 5.15, 3.89, 1.82 for s^+. The same trend shows up for the lithium-halides LiBr, LiCl and LiF where the local softness of halogen atom decreases for both s^- (10.64, 9.56, 7.25) and s^+ (0.91, 0.58, 0.02), in line with what can be expected from the total softness/hardness of the halogens.[11] Moreover, the local softness of carbon in ethane, ethylene and acetylene gives decreases from 2.98 to 2.80 and 0.85 for s^- and from 2.75 to 2.62 and 0.69 for s^+, highlighting the fact that triple bond is softer than double and single bond. All trends align with those in polarizability α,[84, 85] as might be expected from the established relationship between α and S.[86, 87]

Of crucial importance in the present paper, however, is the comparison between the analytically derived Fukui function and the finite difference approximation which has been used as the default method for the past decades. **Fig. 1** displays the results of a detailed comparison between the analytical (**Eqn. 21)** and finite difference atom-condensed Fukui function for benzene and substituted benzenes with -O^-, -NH_2, -OH, -OCH_3, -SH, -$CHCH_2$, -CH_3, -Br, -Cl, -F, COOH, -CHO, -CN and -NO_2 groups, which gained already, in its finite difference approximation, widespread attention from the 1990s on.[88] The computation of the condensed finite difference Fukui function follows **Eqn. 23 and 24**.

$$f_A^- = q_{N-1}^A - q_N^A \tag{23}$$

$$f_A^+ = q_N^A - q_{N+1}^A \tag{24}$$

Where q indicates the charge on the atom A in the N, $N-1$ and $N+1$ electron system respectively. However, **Scheme 1d** shows it is necessary to be aware that benzene has both the two HOMO and LUMO are twofold degenerate so when taking away or adding an electron to the system, symmetry will be broken. Hence, in order to calculate the Fukui function while ensuring a totally symmetric charge distribution (as it should be as the Fukui function is the N-derivative of the totally symmetric electron density), we change two electrons at the same time to form a triplet cation or anion. **Figure 1a** shows the linear correlation

between analytical and finite difference f^- values with correlation coefficient $R^2 = 0.970$ with outliners mainly from carbon atoms at ortho- and meta-position when an electron withdrawing group is attached to the benzene ring. This disagreement can be explained by the different nature in evaluating the Fukui function between analytical and finite difference method. In analogy with the piecewise linear behavior of the energy $E_{N+\lambda}(\boldsymbol{r}) = (1-\lambda)E_N(\boldsymbol{r}) + \lambda E_{N+1}(\boldsymbol{r})$, finally leading to hardness condition (vide supra), the electron density is a linear mixture of the N and $N+1$ densities at fractional charge $N+\lambda$.

$$\rho_{N+\lambda}(\boldsymbol{r}) = (1-\lambda)\rho_N(\boldsymbol{r}) + \lambda\rho_{N+1}(\boldsymbol{r}) \tag{25}$$

with $0 \leq \lambda \leq 1$. For a comprehensive account on this type of relationships and conditions up to third order see **Ref. 87**.[89] Considering the evaluation of the Fukui function at integer N values, the dependence of the chosen frontier orbital f of the analytical expression in **Eqn. 11** confirms its two-side derivative character at integer N (vide supra). The finite difference result, however, uses the slope manipulating the integer N , $N+1$ and $N-1$ ρ values. Taking the N derivative of **Eqn. 25** under the exact functional deriving we obtain

$$f_{N+\lambda}(\boldsymbol{r}) = \rho_{N+1}(\boldsymbol{r}) - \rho_N(\boldsymbol{r}) \tag{26}$$

showing that the two methods are identical. To have a first look at the influence of delocalization error, for $E = E(N)$, **Table S1** gives the hardness conditions for the systems studied in **Fig. 1**. Most of the electron withdrawing groups (EWG) show larger η^- than the electron donating groups (EDG), except for -CN, which corresponds to the outliers in **Fig. 1a** of f^-. Note that f^- is in fact the most important Fukui function to be considered in view of the nature of its most typical reaction, the electrophilic substitution.[88] For almost all substituents, similar and relatively small η^+ values are obtained that parallels the strong correlation of f^+ in **Fig. 1b** where the outlier, pertaining the O^- substituent, can of course be explained by the unstable double anion needed in the evaluation of the finite difference calculation. Note however that the analytical procedure can be applied in this case. **Figure 2** further shows the comparison between fractional occupation from -0.1 to 0.1 (dashed line) and finite difference (solid arrow) calculation at ortho, meta and

para position for selected well- and ill-behaved systems in **Fig. 1**. For well-behaved systems, **Fig. 2a and 2c**, the linearity obtained from fractional occupation is in line with the finite difference method, which indicates the ρ vs N curve is indeed piece-wise linear (**Eqn. 25**) in these cases, and as a result their Fukui functions are similar. As can be seen from **Fig. 2b and 2d**, however, the dashed line is below the solid arrow thus yielding a convex behavior for the ρ vs N curve similar to the E vs N curve, obtained with fractional occupation numbers, which causes the difference between the two approaches in calculating the Fukui function. According to **Eqn. 11** the Fukui function can be written as the difference between the frontier orbital density, and a second term, which is again (cf. the hardness condition discussion) the result of a matrix product $\mathbf{K}_{\mathbf{ia}}^{\mathbf{T}}\mathbf{M}_{\mathbf{ia},\mathbf{jb}}\mathbf{S}_{\mathbf{jb}}$ involving al orbitals, occupied and unoccupied. This situation was already implicitly put forward in an alternative approach by Yang, Parr and Pucci,[90] writing the Fukui function as a frontier orbital density term, the analogue of the frontier orbital approach of the hardness in **Eqn. 2**, followed by a correction term involving orbital N-derivatives. Since in practice the frontier orbital density term is usually much larger in value than the second one, the overall result might indicate that the Fukui function might be less sensitive to the delocalization error than the hardness.

So, how to choose between the analytical and finite difference method in chemical reactivity studies?

Let us start from the fact that when the exact functional is applied both the finite difference and the analytical method should give the same results due to the Fukui function condition **Eqn. 26.** If the DFA, however, can give exact or highly accurate density for neutral and charged states the finite difference approach can then be preferable for practical reasons, though requiring two calculations. On the other hand, DFAs with minor (de)localization error are qualified for analytical investigations. So, the rule of thumb for the Fukui function evaluation: practically and in general, the finite difference approach should be more preferred except for the study of negatively charged systems (f^+ for anion) i.e., phenoxide ion in **Fig. 1b** where the analytical method is more reliable as discussed above. A combined evaluation of the finite difference and analytical Fukui function may be recommended giving insight in the way the

delocalization error affects the electron density. Going one step further the second order N-derivative of electron density $\frac{\delta^3 E}{\partial N^2 \delta v(\boldsymbol{r})} = \frac{\delta^2 \rho(\boldsymbol{r})}{\partial N^2}$ i.e., the dual descriptor $f^{(2)}(\boldsymbol{r})$ in **scheme 1b**.[19, 20] might give further information on the (de)localization error with its the dual descriptor condition[89] $f^{(2)^{\pm}}(\boldsymbol{r}) = 0$ for non-integer N values similar to the hardness condition $\eta^{\pm}$ discussed in previous section Overall, the conditions for local descriptors contain richer information in their conditions as they are to be satisfied at each $\boldsymbol{r}$, or even going further each $\boldsymbol{r}$ and $\boldsymbol{r}$' combination.[89]

In analogy with the hardness, one, however, evidently can keep the chemistry of the well-known and widely accepted dual descriptor, by considering the finite different approximation[19, 20, 91] and evaluate the dual descriptor by the difference between the f^+ and f^- yielding $f^{(2)}(\boldsymbol{r}) = \rho_{N+1}(\boldsymbol{r}) - 2\rho_N(\boldsymbol{r}) + \rho_{N-1}(\boldsymbol{r})$ in analogy with the finite difference expression for the hardness (**Eqn. 1**).

4.3 Softness kernel and nearsightedness revisited

The softness kernel, defined as the derivative of the electron density with respect to the external potential at fixed electronic chemical potential, matches closely the concept of the nearsightedness of electronic matter (NEM), where it is stated that at fixed chemical potential the electron density at a point $\boldsymbol{r_0}$ cannot "see" any perturbation at a point $\boldsymbol{r}$' beyond a given radius R with an accuracy larger than $\Delta\rho$, this value being a function of $\boldsymbol{r_0}$ and R, no matter how large the perturbation is. For systems with a non-zero band gap (or chemical hardness) this leads to an exponential decay of the density as a function of the distance between the point at which the perturbation is placed, $\boldsymbol{r_0}$ and another point $\boldsymbol{r}$. In the previous work this "physics" NEM principle was reconciled with the chemist's transferability of functional groups[92] via the softness kernel with a few examples. In the present work extend the evaluation of softness kernel in the framework of analytical CDFT given above and provide some extra examples.[41] Since for N-derivatives CDFT response properties are evaluated separately at the electron abundant and deficient side, converting the linear response function using the Berkowitz-Parr relation (**Eqn. 22**) gives rise to two softness kernels,

one from the electron deficient side $s^-(\boldsymbol{r},\boldsymbol{r}')$ and another from the electron abundant side $s^+(\boldsymbol{r},\boldsymbol{r}')$. For reasons of internal consistency, in an expression where sums of terms and products of factors are used, we always use the hardness condition when adopting the Berkowitz-Parr relation as we will also do in the evaluation of the hardness kernel in section 4.4. For efficiency reasons, all calculations reported below employ the PBE/cc-pVDZ level of theory where the evaluation of the $f_{xc}(\boldsymbol{r},\boldsymbol{r}')$ kernel for CDFT properties is performed without considering the density gradient terms. **Figure 3** shows the condensed softness kernel results for homologous series of 1-hydroxy substituted linear alkanes and polyenes within the latter case a saturating methyl group at the end of the chain. Detailed numerical results are presented in **Table S2 and S3**. Though showing oscillations along the alkene chain **Fig. 3a and 3b**, the case of the longest chain (13 carbon atoms, n=6) reveals that the influence of the hydroxyl group along the chain, measured by considering the s_{O,C_n} softness kernel elements, is already strongly diminished after two carbons and nearly vanishes at positions further from the perturbation, but for the s^+ and s^- kernels. (The s^+ being chemically more interesting in view of the dominating mesomeric donor character of the OH group). The lower members of the homologous series hardly differ in their behavior except for a very slight, numerically unimportant rise, at the end of the chain which nicely converges to 0 for the largest chain (see insert). A similar behavior, shown in **Fig. 3c and 3d**, is observed in the saturated chains where the nearsightedness is now almost reached after one carbon, and the "edge effect" at the end of the chain is even much smaller than in the polyene case. Again, the two (HOMO and LUMO based) expression of the softness kernel $s^-(\boldsymbol{r},\boldsymbol{r}')$ and $s^+(\boldsymbol{r},\boldsymbol{r}')$ show the same extremely "local" behavior. The difference in faster decay in the alkane case can be traced back to the "inductive-only" effect (in fact the s^- kernel is here more relevant) as compared to the inductive plus mesomeric effect in the polyene, knowing that an OH group has a stronger mesomeric donor than inductive acceptor effect. As a comparison **Fig. 2S** gives the evolution of the linear response function χ_{O,C_n} for the same systems where the decrease in value is not as fast as in the softness kernel since it is not nearsighted as being evaluated not at constant electronic

chemical potential but at constant number of electrons in line with the very little data already available (2 refs). The complete set of LRF data on the present studies is given in **Table S4**. Overall, our results are a further support[29, 41] for the chemical translation of the Nearsightedness of Electronic Matter principle as the electron density cannot "see" any more the change of external potential after a small number of carbons atoms.

4.4 Hardness kernel and electron population normal modes

Having access to the softness kernel, the hardness kernel can be obtained by inverting the softness kernel. The evaluation of the hardness kernel is, however, mathematically problematic since, the softness kernel can have very small eigenvalues (e.g., upon extending the basis set the lowest eigenvalue is tending more to zero or even becomes zero, the kernel then becoming non-invertible (for a detailed discussion see **Ref. 22**). The problem can be avoided starting from the atom condensed version of the softness kernel yielding a condensed hardness kernel or hardness matrix $\boldsymbol{\eta}_{\boldsymbol{AB}}^{\pm}$ as its inverse. Note that just as in the case of the softness matrix, two hardness matrices are obtained with the present ansatz. The properties of this matrix were extensively studied by Nalewajski and coworkers in the context of their charge sensitivity analysis (CSA)[46, 47] by using a semiempirical ansatz based on Mortier's Electronegativity Equalization method.[48] The present paper offers the possibility to retake this line of research but now starting from high quality DFA calculations. A key concept in Nalewajski's work are the normal modes of electron population displacements, in short, the(electron) population normal modes (PNMs) of a system, defined, within the atoms-in-molecules resolution, as the eigenvectors $\boldsymbol{U_r}$ of the hardness matrix. The corresponding eigenvalues h_r are termed the principal hardness values and can be degenerate: more than one of the PNMs can correspond to a given h. Note that the eigenvalues of the hardness matrix are the inverse of those of the softness in view of relationship $\boldsymbol{s} = \boldsymbol{\eta}^{-1}$.[22, 46] The eigenvectors can be grouped in an orthogonal matrix $\boldsymbol{U}$ which diagonalizes the hardness matrix $\boldsymbol{\eta}$

$$\boldsymbol{U^T \eta\, U = h},\ (\boldsymbol{U^T U = I}) \tag{27}$$

It turns out that PNMs can be categorized into charge transfer (CT) modes which deal with an overall in- or out-flow of electrons in/out of the system or polarization (P) modes with purely internal redistributions of electrons.

Table 3 gives the two condensed hardness kernels or matrices $\boldsymbol{\eta_{AB}^{\pm}}$ obtained by inverting the condensed softness kernel or matrix, and all PNMs with decreasing principal hardness h in the case of the H_2O molecule. The corresponding Nalewajski diagrams of the PNMs are shown in **Fig. 4** with the same sequence as the principal hardness in **Table 3**, where white and black circles stand for inflow and outflow of electrons respectively with the circle radius indicating the relative magnitude of such changes. Our results agree qualitatively with the one obtained by Nalewajski's EEM based approach.[46] The symmetry is identical. The differences in circle radius are a consequence of the difference in level of theory between the original EEM method and the present "analytical" DFT ansatz. In the case of $\boldsymbol{\eta_{AB}^{-}}$ two PNMs belong to the totally symmetric representation A_1 of the $\mathrm{C}_{2\mathrm{V}}$ point-group, one to B_1 as should be according to a symmetry analysis. That the PNM with highest principal hardness belongs to the totally symmetric representation was also found by Nalewajski. Moreover, all PNMs show the same overall characteristics as in Nalewajski's work, though, of course, the picture is more refined through the appearance of two hardness matrices. For $\boldsymbol{\eta_{AB}^{-}}$ it is not surprising that at this electron deficient side the softest mode (**Fig. 4** top right) illustrates the oxygen tendency to donate electrons. On the other hand, the electron abundant side $\boldsymbol{\eta_{AB}^{+}}$ shows an inversion in symmetry with the softest mode (**Fig. 4** lower right) being totally symmetric and where the hydrogens are likely to take electrons in this Charge Transfer type mode. That is consistent with the fact that upon reaction, the oxygen atom is usually the electron donor, and because of its high electronegativity, the nearby hydrogens, which are acidic, have the potential to gain electrons. A second example of the representation of the PNMs for the two condensed hardness kernels can be found for pyrrole in **Table S5** and **Fig. S3** where similar interpretation can be applied. The new analytical formulation

of conceptual DFT provides a straightforward and clear access to the PNMs and related CSA concepts in a more refined view. With the two hardness matrices, it is now possible to scrutinize chemical reactivity with dedicated PNMs on both the electron deficient and abundant side.

4.5 Perturbation expansion and energy decomposition

Conceptual DFT and its response descriptors are widely known from its perturbative formulation, here written up to second order[3, 11]

$$E[N+\Delta N, v+\Delta v] = E[N,v] + \left(\frac{\partial E}{\partial N}\right)_v \Delta N + \int \left(\frac{\partial E}{\delta v(\boldsymbol{r})}\right)_N \Delta v(\boldsymbol{r}) d\boldsymbol{r} + \frac{1}{2}\left(\frac{\partial^2 E}{\partial N^2}\right)_v \Delta N^2$$
$$+\Delta N \int \frac{\partial^2 E}{\partial N \delta v(\boldsymbol{r})} \Delta v(\boldsymbol{r}) d\boldsymbol{r} + \frac{1}{2}\int \left(\frac{\partial^2 E}{\delta v(\boldsymbol{r}) \delta v(\boldsymbol{r}')}\right)_N \Delta v(\boldsymbol{r}) \Delta v(\boldsymbol{r}')\, d\boldsymbol{r} d\boldsymbol{r}' + \cdots \quad (28)$$

where the energy difference induced by changes in N and $v(\boldsymbol{r})$ is formulated using a Taylor expansion in which the response functions discussed above appear in a natural way.

In 1997, Liu and Parr[49-51] proposed another expansion method within the framework of conceptual DFT by means of a functional expansion of the total energy, which, however, has not yet been thoroughly investigated yet. **Eqn. 29** gives this functional expansion of the total energy in the canonical ensemble up to second order

$$E[N,v] = Const. + \left(\frac{\partial E}{\partial N}\right)_v N + \int \left(\frac{\partial E}{\delta v(\boldsymbol{r})}\right)_N v(\boldsymbol{r}) d\boldsymbol{r} - \frac{1}{2}\left(\frac{\partial^2 E}{\partial N^2}\right)_v N^2$$
$$-N \int \frac{\partial^2 E}{\partial N \delta v(\boldsymbol{r})} v(\boldsymbol{r}) d\boldsymbol{r} - \frac{1}{2}\int \left(\frac{\partial^2 E}{\delta v(\boldsymbol{r}) \delta v(\boldsymbol{r}')}\right)_N v(\boldsymbol{r}) v(\boldsymbol{r}')\, d\boldsymbol{r} d\boldsymbol{r}' + \cdots \quad (29)$$

Remark similarities (appearance of the CDFT response functions) and differences (signs of the second order terms) with **Eqn. 28**. Furthermore, a constant appears which is not necessarily zero and depends on the system. On the basis of **Eqn. 29** the total electronic energy — not its change under perturbation as in **Eqn. 28** — can be decomposed into a sum of products and integrals involving CDFT descriptors. Each term on the right-hand side of **Eqn. 29** corresponds to different-energy contributions, which gives rise to a new energy decomposition approach (EDA) based on conceptual DFT (CDFT-EDA).

$$E[N,v] = Const. + E_\mu + E_\rho + E_\eta + E_f + E_\chi + \cdots \quad (30)$$

where the identification of the terms is made by the corresponding response function. As first order N-derivatives may be considered both from the electron abundant and the electron deficient side, the corresponding (+/- superscripted) energy contributions, for example E_μ and E_f, should be used for considering the energy *evolution* upon perturbation of the number of electrons from the electron abundant or deficient side respectively. For the exact functional under 0K limit, the energetic contribution of (mixed) second- or higher-order N-derivatives reduces to zero ($E_\eta^\pm$). Unlike other EDAs (from Morokuma's schemes presented in the 1970s[93] to the Ziegler-Rauk energy decomposition analysis,[94] as adopted among others in Bickelhaupt's Activation Strain Model[95] and Head-Gordon's EDA based on absolute localized molecular orbitals[96] and many others …) that divide the interaction energy into a very limited number of contributions, CDFT-EDA expands the total energy into an infinite number of terms whose convergence should be investigated, though earlier considerations on its perturbation analogue **Eqn. 28** give indications that already a second order expansion as shown in **Eqn. 29** most probably might yield satisfactory results.[8] Though through the appearance of the unknown constant term in **Eqn. 30** a perfect numerical equivalence between the left- and right-hand side of **Eqn. 30** cannot be envisaged, the power of **Eqn. 30** is that all other energy contributions from the right-hand side of the equation have a clear chemical interpretation, and therefore the chemical significance of **Eqn. 30** should come from the investigation of each energetic contribution of conceptual DFT, i.e. from comparing *relative* contributions. Remark that the expression in **Eqn. 29** from the left and the right (electron deficient and abundant side) should converge to the same energy value if the expansion is complete. The identification of the terms yield, for the pure v-derivative terms, E_ρ as the electron-nuclear interaction energy and E_χ as the polarization energy. The preponderant role of the linear response function in polarization phenomena has been known for some time and recently stressed by the present authors.[97] The first order (mixed) N-

derivative term can be re-written as N times the derivative of the electrostatic component E_ρ with respect to N.

$$N\int \frac{\partial^2 E}{\partial N \delta v(\boldsymbol{r})} v(\boldsymbol{r}) d\boldsymbol{r} = N\int \frac{\partial}{\partial N}[\rho(\boldsymbol{r})v(\boldsymbol{r})]d\boldsymbol{r} = N\frac{\partial E_\rho}{\partial N} \quad (31)$$

In other words, the sensitivity of the electron-nuclear interaction energy to changes in the number of electrons. Finally, the first pure N term, involving the electronic chemical potential bears strong similarity to the Gibbs free energy expression for a single component system written as n (number of moles) times the chemical potential,[98] replaced here by N (number of electrons) times the chemical potential. Coming back to the hardness term: in view of the preceding sections the hardness conditions should be used and similarly for the higher order N terms[89] (hyperhardness etc. where the corresponding conditions again impose a zero value for non-integer N) so that, in a natural way, the series does not blow up for large N.

In **Table 4** we give the values for the different energy components for a few di-atomic and 10-electron systems at the equilibrium geometry where the hardness condition values are inserted, again for reasons of internal consistency. It is seen that the terms involving pure v derivatives, the electron-nuclear interaction energy and the polarization energy are strongly dominating, illustrating the importance of the linear response function in evaluating/discussing this type of schemes. The mixed N and v i.e., Fukui terms are, as compared to the LRF is smaller but still important, on the average 50% of that term, their difference between left and right derivative being non-negligible. With all reservations expressed above on the hardness term, its contribution on its turn is at most 50% of the Fukui function term. Finally, the chemical potential term is by far the smallest one, being, very roughly, one or even two orders of magnitude smaller than the other first order N- derivative term, E_f. Further research is needed to scrutinize trends in order of magnitude. Similar trends are found in the complete series, with a remarkable similarity between the two iso-electronic molecules CO and N_2. Also, the 10-electron molecules show similar trends, most terms, in absolute value, show an increasing trend from CH_4, NH_3, H_2O to HF. The strong increase in value when passing from HF, to HCl and HBr reflects the increasing polarizability of the

halogen (cf. section 4.1), whose role in the total energy expression is taken care of by the linear response function (see also our recent findings on the role of the LRF in halogen bonds)[97] Further research, now that the conceptual and computational tools are available, should be performed in order to get a more refined view on this CDFT based energy decomposition. An open question that remains is how to interpret the sign differences in the second order terms in the functional expansion as compared to the perturbation expansion and give it a physical/chemical justification.

As an outlook we present an example of a different type considering the *evolution* of these energy components upon a chemical process. **Fig. 5** illustrates changes of the different energy components upon bond stretching (up to 1.0Å) and compression (up to 0.3Å) of hydrogen fluoride with respect to equilibrium. As can be seen from the figure starting from the left in **Fig. 5**, upon increasing bond length the electronic energy E_{el}, and its components E_{μ^-}, E_{ρ}, E_{f^-} rise, while E_{η^-} (for DFAs only) decreases whereas the E_{χ} curve shows a maximum. Judging the relative contribution of each energy component, the N-derivative terms are much smaller, one order of magnitude, than the v-derivative terms, not unexpected in view of the nature of the perturbation, which is a Δv perturbation. The electron-nuclear interaction energy E_{ρ} and electron polarization energy E_{χ} both experience a rapid increase before the equilibrium distance is attained or, to put it otherwise, strongly decrease when the bond is compressed. Their opposite behavior for elongations larger than 0.2Å eventually leads to a slow rise in the total electronic energy at large distance. The mixing, Fukui function term, is, not unexpectedly, in the middle range of the pure N and v contributions. **Figure 6** displays another chemical process characterized by a Δv perturbation now driven by variation in angle: the dihedral rotation of H_2O_2 where the angle variation modulates steric effects. From the figure we observe that as the dihedral angle increases from 0 to 180 degrees, the by far most important and dominant change is the second order pure v polarization term E_{χ} the first order pure or mixed v-terms, E_{ρ} and E_{f^-} again being similar in magnitude as in the previous case but contributing much less to the overall energy change.

Returning finally to the perturbation expansion **(Eqn. 28)** the availability of all response functions at the same level of theory and the integration techniques described in Section 3 enables us to numerically evaluate all terms of the perturbation expansion up to second order for perturbations in v or/and N. We again concentrate on HF by evaluating the total energy difference ΔE of the hydrogen fluoride bond upon stretching from the equilibrium distance by 0.1Å in steps of 0.01Å while simultaneously changing the number of (fractional) electrons from 0 to -1 and from 0 to +1. We thereby adopt the conventions for electron abundant and deficient sides in the notation and the insertion of the appropriate response functions in **Eqn. 28.** Where in **Fig. 7** we compare the $\Delta E_{el}(CDFT^{-})$ and $\Delta E_{el}(CDFT^{+})$ values with the electronic energy denoted as ΔE_{el} obtained by a DFA calculations at the PBE/cc-pVTZ level of theory with fractional number of electrons. The ΔE_{el} surface is indicated with a blue-white-red color code, whereas the brown-white-green surface represents the $\Delta E_{el}(CDFT)$ obtained with the CDFT perturbation expansion up to second order in **Eqn. 28** both for the electron abundant and deficient sides. The energy surface approximated from perturbation expansion based on the HOMO orbital $\Delta E_{el}(CDFT^{-})$ gives an excellent result, better than LUMO orbital based $\Delta E_{el}(CDFT^{+})$ when comparing with the DFA ΔE_{el}surface, though the $E_{el}(CDFT^{+})$ is still very reasonable.

The quality of the $CDFT^{-}$ results can be judged by observing in **Fig. 7a** the two surfaces are almost completely overlapping so that one of them is nearly invisible. Numerically, the mean absolute error between the energy values for all 121 data points is only 0.27eV with the maximum error equals to 0.89eV. This result is into the best of our knowledge one of the first, numerical, examples to show how in the case of small perturbations, the perturbation series up to second order, in particular $E_{el}(CDFT^{-})$ already predicts very reasonable energy changes. The larger deviation for $E_{el}(CDFT^{+})$ is in line with many observations that the electron abundant side is less well described in CDFT due to the less accurate description of the LUMO as compared to the HOMO.

Summarizing the findings in this section, expansions **Eqn. 28 and 30** provide alternative and complementary views on the CDFT decomposition of the energy and its changes upon perturbations as occurring in chemical process which can, at least in principle, be refined by including higher order terms for which analytical expressions for the corresponding response functions have been formulated.[89]

5. Conclusion

We have presented the basic equations for analytical conceptual DFT up to the second order, and then conducted a comparative study with the frontier orbital approximation and finite different approach that have been widely used in the past decades. The role and the intricacies of the different conditions resulting from the piecewise linear behavior of the $E = E(N)$ curve in this endeavor were highlighted, in particular for the hardness. The essential difference in the physical/chemical meaning between the Parr-Pearson chemical hardness and the hardness condition is stressed. The latter offers a unique ability of evaluating the (de)localization error in DFAs connecting with literature data. On the other hand, numerical results for both the analytical and finite difference Fukui functions were shown to display, in most cases, only small differences in a series substituted benzene. Further insight into the error was gained by testing the linearity of ρ vs N curve using fractional occupation number calculations. For general practical purposes, the finite difference approach should be preferable, except for evaluating the Fukui function for negatively charged systems. The nearsightedness of electronic matter was revisited with the softness kernel for 1-OH linear alkane and polyene chains. The substitution effect along the carbon chain was retrieved both for the inductive and mesomeric effect. Due to nearsightedness the softness kernel exhibited extremely "local" behavior compared to the linear response function, drastically converging to zero after one or two carbon atoms. As a side result an extension was made by inverting the condensed softness kernel, to obtain the hardness matrix, yielding after diagonalization high level values for the corresponding analytical principal hardness and population normal modes of Nalewajski's charge sensitivity analysis. Finally, two approaches for conceptual DFT based energy expansion were scrutinized based on numerical values for each term up to second order thereby combining the analytical expressions for the response functions and the numerical integration tools. One is the well-known perturbation expression, and the other one is the functional Taylor expansion which hitherto received less attention. The latter one was used to set up a new, conceptual DFT based, energy decomposition scheme. A case study on diatomics and the well-known

series of ten-electron molecules showed that the energy components in this functional Taylor expansion contain potentially important information about molecular energetics, highlighting for example the importance of v-dependent terms. On the other hand, the perturbation expansion up to second order gave already fine results when compared to the electronic energy calculated via fractional occupation number. Both numerical studies are the first of their kind in the literature. Therefore, efforts in numerical studies should continuously be pursued to extract firmly based chemical insight from these energy decompositions.

Summarizing, our results coming from analytical conceptual DFT not only provide new tools for reactivity studies including numerical data but also may be instrumental in scrutinizing the accountability of DFAs in DFT developments as such.

6. ACKNOWLEDGEMENTS

FDP acknowledges support of the Vrije Universiteit Brussel through a Strategic Research Program awarded to his research group. FDP and BW further acknowledge the Research Foundation Flanders (FWO) for financial support, among others through SBO research grant S003818N. BW acknowledges the support from Chinese Scholarship Council (No. 202106720017). BW also wants to thank Prof. Weitao Yang from Duke university for the private conversations about hardness condition in DFT2022 and ICQC2023 conferences.

7. ASSOCIATED CONTENT

Supporting information contains the following contents:

a. Supplementary Tables and Figures mentioned in this article.

b. Cartesian coordinates of systems studied in this article.

8. REFERENCES

(1) Parr, R. G.; Yang, W. Density-functional theory of the electronic structure of molecules. *Annu. Rev. Phys. Chem.* **1995**, *46* (1), 701-728.
(2) Chermette, H. Chemical reactivity indexes in density functional theory. *J. Comput. Chem.* **1999**, *20* (1), 129-154.
(3) Geerlings, P.; De Proft, F.; Langenaeker, W. Conceptual density functional theory. *Chem. Rev.* **2003**, *103* (5), 1793-1874.
(4) Ayers, P. W.; Anderson, J. S. M.; Bartolotti, L. J. Perturbative perspectives on the chemical reaction prediction problem. *Int. J. Quantum Chem.* **2005**, *101* (5), 520-534.
(5) Gázquez, J. L. Perspectives on the density functional theory of chemical reactivity. *J. Mex. Chem. Soc.* **2008**, *52* (1), 3-10.
(6) Geerlings, P.; De Proft, F. Conceptual DFT: The chemical relevance of higher response functions. *Phys. Chem. Chem. Phys.* **2008**, *10* (21), 3028-3042.
(7) Liu, S. Conceptual density functional theory and some recent developments. *Acta Phys. -Chim. Sin.* **2009**, *25* (3), 590-600.
(8) Geerlings, P.; Chamorro, E.; Chattaraj, P. K.; De Proft, F.; Gázquez, J. L.; Liu, S.; Morell, C.; Toro-Labbé, A.; Vela, A.; Ayers, P. W. Conceptual density functional theory: Status, prospects, issues. *Theor. Chem. Acc.* **2020**, *139* (2), 36.
(9) Liu, S. *Conceptual Density Functional Theory: Towards a New Chemical Reactivity Theory*; Wiley-VCH, 2022.
(10) Parr, R. G.; Donnelly, R. A.; Levy, M.; Palke, W. E. Electronegativity: The density functional viewpoint. *J. Chem. Phys.* **1978**, *68* (8), 3801-3807.
(11) Parr, R. G.; Yang, W. *Density-Functional Theory of Atoms and Molecules*; Oxford University Press, 1989.
(12) Mulliken, R. S. A new electroaffinity scale; Together with data on valence states and on valence lonization potentials and electron affinities. *J. Chem. Phys.* **1934**, *2* (11), 782-793.
(13) Parr, R. G.; Pearson, R. G. Absolute hardness: Companion parameter to absolute electronegativity. *J. Am. Chem. Soc.* **1983**, *105* (26), 7512-7516.
(14) Pearson, R. G. *Chemical Hardness: Applications from Molecules to Solids*; Wiley-VCH, 1997.
(15) Martin, R. M. *Electronic Structure: Basic Theory and Practical Methods*; Cambridge University Press, 2012.
(16) Senet, P. Kohn-Sham orbital formulation of the chemical electronic responses, including the hardness. *J. Chem. Phys.* **1997**, *107* (7), 2516-2524.
(17) Parr, R. G.; Yang, W. Density functional approach to the frontier-electron theory of chemical reactivity. *J. Am. Chem. Soc.* **1984**, *106* (14), 4049-4050.
(18) Yang, W.; Parr, R. G. Hardness, softness, and the fukui function in the electronic theory of metals and catalysis. *Proc. Natl. Acad. Sci. U. S. A.* **1985**, *82* (20), 6723-6726.
(19) Morell, C.; Grand, A.; Toro-Labbé, A. New dual descriptor for chemical reactivity. *J. Phys. Chem. A* **2005**, *109* (1), 205-212.
(20) Morell, C.; Grand, A.; Toro-Labbé, A. Theoretical support for using the Δf(r) descriptor. *Chem. Phys. Lett.* **2006**, *425* (4), 342-346.
(21) Geerlings, P.; Fias, S.; Boisdenghien, Z.; De Proft, F. Conceptual DFT: Chemistry from the linear response function. *Chem. Soc. Rev.* **2014**, *43* (14), 4989-5008.
(22) Fias, S.; Ayers, P. W.; De Proft, F.; Geerlings, P. Properties of the density functional response kernels and its implications on chemistry. *J. Chem. Phys.* **2022**, *157* (11), 114102.
(23) Ullrich, C. A. *Time-Dependent Density-Functional Theory: Concepts and Applications*; Oxford University Press, 2011.

(24) Runge, E.; Gross, E. K. U. Density-functional theory for time-dependent systems. *Phys. Rev. Lett.* **1984**, *52* (12), 997-1000.
(25) Grabo, T.; Petersilka, M.; Gross, E. K. U. Molecular excitation energies from time-dependent density functional theory. *Journal of Molecular Structure: THEOCHEM* **2000**, *501-502*, 353-367.
(26) Boisdenghien, Z.; Fias, S.; Da Pieve, F.; De Proft, F.; Geerlings, P. The polarisability of atoms and molecules: A comparison between a conceptual density functional theory approach and time-dependent density functional theory. *Mol. Phys.* **2015**, *113* (13-14), 1890-1898.
(27) Casida, M. E. Time-Dependent Density Functional Response Theory for Molecules. In *Recent Advances in Density Functional Methods*, 1995; pp 155-192.
(28) Casida, M. E. Time-dependent density-functional theory for molecules and molecular solids. *Journal of Molecular Structure: THEOCHEM* **2009**, *914* (1), 3-18.
(29) Wang, B.; Geerlings, P.; Van Alsenoy, C.; Heider-Zadeh, F.; Ayers, P. W.; De Proft, F. Investigating the linear response function under approximations following the coupled-perturbed approach for atoms and molecules. *J. Chem. Theory Comput.* **2023**, *19* (11), 3223-3236.
(30) Boisdenghien, Z.; Van Alsenoy, C.; De Proft, F.; Geerlings, P. Evaluating and interpreting the chemical relevance of the linear response kernel for atoms. *J. Chem. Theory Comput.* **2013**, *9* (2), 1007-1015.
(31) Boisdenghien, Z.; Fias, S.; Van Alsenoy, C.; De Proft, F.; Geerlings, P. Evaluating and interpreting the chemical relevance of the linear response kernel for atoms II: Open shell. *Phys. Chem. Chem. Phys.* **2014**, *16* (28), 14614-14624.
(32) Fias, S.; Boisdenghien, Z.; De Proft, F.; Geerlings, P. The spin polarized linear response from density functional theory: Theory and application to atoms. *J. Chem. Phys.* **2014**, *141* (18), 184107.
(33) Sablon, N.; De Proft, F.; Geerlings, P. The linear response kernel: Inductive and resonance effects quantified. *J. Phys. Chem. Lett.* **2010**, *1* (8), 1228-1234.
(34) Fias, S.; Geerlings, P.; Ayers, P.; De Proft, F. σ, π aromaticity and anti-aromaticity as retrieved by the linear response kernel. *Phys. Chem. Chem. Phys.* **2013**, *15* (8), 2882-2889.
(35) Sablon, N.; De Proft, F.; Solà, M.; Geerlings, P. The linear response kernel of conceptual DFT as a measure of aromaticity. *Phys. Chem. Chem. Phys.* **2012**, *14* (11), 3960-3967, 10.1039/C2CP23372J.
(36) Fias, S.; Boisdenghien, Z.; Stuyver, T.; Audiffred, M.; Merino, G.; Geerlings, P.; De Proft, F. Analysis of aromaticity in planar metal systems using the linear response kernel. *J. Phys. Chem. A* **2013**, *117* (16), 3556-3560.
(37) Sablon, N.; De Proft, F.; Geerlings, P. The linear response kernel of conceptual DFT as a measure of electron delocalisation. *Chem. Phys. Lett.* **2010**, *498* (1), 192-197.
(38) Stuyver, T.; Fias, S.; De Proft, F.; Fowler, P. W.; Geerlings, P. Conduction of molecular electronic devices: Qualitative insights through atom-atom polarizabilities. *J. Chem. Phys.* **2015**, *142* (9), 094103.
(39) Kohn, W. Density functional and density matrix method scaling linearly with the number of atoms. *Phys. Rev. Lett.* **1996**, *76* (17), 3168-3171.
(40) Prodan, E.; Kohn, W. Nearsightedness of electronic matter. *Proc. Natl. Acad. Sci. U. S. A.* **2005**, *102* (33), 11635-11638.
(41) Fias, S.; Heidar-Zadeh, F.; Geerlings, P.; Ayers, P. W. Chemical transferability of functional groups follows from the nearsightedness of electronic matter. *Proc. Natl. Acad. Sci. U. S. A.* **2017**, *114* (44), 11633-11638.
(42) Berkowitz, M.; Parr, R. G. Molecular hardness and softness, local hardness and softness, hardness and softness kernels, and relations among these quantities. *J. Chem. Phys.* **1988**, *88* (4), 2554-2557.
(43) Yang, W.; Cohen, A. J.; De Proft, F.; Geerlings, P. Analytical evaluation of Fukui functions and real-space linear response function. *J. Chem. Phys.* **2012**, *136* (14), 144110.
(44) Perdew, J. P.; Parr, R. G.; Levy, M.; Balduz, J. L. Density-functional theory for fractional particle number: Derivative discontinuities of the energy. *Phys. Rev. Lett.* **1982**, *49* (23), 1691-1694.

(45) De Proft, F.; Liu, S.; Parr, R. G. Chemical potential, hardness, hardness and softness kernel and local hardness in the isomorphic ensemble of density functional theory. *J. Chem. Phys.* **1997**, *107* (8), 3000-3006.
(46) Nalewajski, R. F.; Korchowiec, J.; Zhou, Z. Molecular hardness and softness parameters and their use in chemistry. *Int. J. Quantum Chem.* **1988**, *34* (S22), 349-366.
(47) Nalewajski, R. F. Normal (decoupled) representation of electronegativity equalization equations in a molecule. *Int. J. Quantum Chem.* **1991**, *40* (2), 265-285.
(48) Mortier, W. J.; Leuven, K. U. Electronegativity equalization and its applications. In *Structure and Bonding*, Sen, K. D., Jørgensen, C. K. Eds.; Vol. 66; Springer Berlin Heidelberg, 1987; pp 125-143.
(49) Parr, R. G.; Liu, S.; Kugler, A. A.; Nagy, Á. Some identities in density-functional theory. *Phys. Rev. A* **1995**, *52* (2), 969-976.
(50) Liu, S. Local-density approximation, hierarchy of equations, functional expansion, and adiabatic connection in current-density-functional theory. *Phys. Rev. A* **1996**, *54* (2), 1328-1336.
(51) Liu, S.; Parr, R. G. Second-order density-functional description of molecules and chemical changes. *J. Chem. Phys.* **1997**, *106* (13), 5578-5586.
(52) Mori-Sánchez, P.; Cohen, A. J.; Yang, W. Localization and delocalization errors in density functional theory and implications for band-gap prediction. *Phys. Rev. Lett.* **2008**, *100* (14), 146401.
(53) Cook, D. B. *Handbook of Computational Quantum Chemistry*; Dover Publications, 2005.
(54) Kohn, W.; Sham, L. J. Self-consistent equations including exchange and correlation effects. *Phys. Rev.* **1965**, *140* (4A), A1133-A1138.
(55) Perdew, J. P.; Schmidt, K. Jacob's ladder of density functional approximations for the exchange-correlation energy. *AIP Conf. Proc.* **2001**, *577* (1), 1-20.
(56) Teale, A. M.; Helgaker, T.; Savin, A.; Adamo, C.; Aradi, B.; Arbuznikov, A. V.; Ayers, P. W.; Baerends, E. J.; Barone, V.; Calaminici, P.; et al. DFT exchange: Sharing perspectives on the workhorse of quantum chemistry and materials science. *Phys. Chem. Chem. Phys.* **2022**, *24* (47), 28700-28781, 10.1039/D2CP02827A.
(57) Bultinck, P.; Clarisse, D.; Ayers, P. W.; Carbo-Dorca, R. The Fukui matrix: A simple approach to the analysis of the Fukui function and its positive character. *Phys. Chem. Chem. Phys.* **2011**, *13* (13), 6110-6115, 10.1039/C0CP02268C.
(58) Liu, S.; De Proft, F.; Parr, R. G. Simplified models for hardness kernel and calculations of global hardness. *J. Phys. Chem. A* **1997**, *101* (37), 6991-6997.
(59) Lee, C.; Yang, W.; Parr, R. G. Development of the Colle-Salvetti correlation-energy formula into a functional of the electron density. *Phys. Rev. B* **1988**, *37* (2), 785-789.
(60) Becke, A. D. Density-functional exchange-energy approximation with correct asymptotic behavior. *Phys. Rev. A* **1988**, *38* (6), 3098-3100.
(61) Stephens, P. J.; Devlin, F. J.; Chabalowski, C. F.; Frisch, M. J. Ab Initio calculation of vibrational absorption and circular dichroism spectra using density functional force fields. *J. Phys. Chem.* **1994**, *98* (45), 11623-11627.
(62) Dunning, T. H., Jr. Gaussian basis sets for use in correlated molecular calculations. I. The atoms boron through neon and hydrogen. *J. Chem. Phys.* **1989**, *90* (2), 1007-1023.
(63) Frisch, M.; Trucks, G.; Schlegel, H.; Scuseria, G.; Robb, M.; Cheeseman, J.; Scalmani, G.; Barone, V.; Petersson, G.; Nakatsuji, H. Gaussian 16. Gaussian, Inc. Wallingford, CT: 2016.
(64) Perdew, J. P.; Burke, K.; Ernzerhof, M. Generalized gradient approximation made simple. *Phys. Rev. Lett.* **1996**, *77* (18), 3865-3868.
(65) Sun, Q.; Berkelbach, T. C.; Blunt, N. S.; Booth, G. H.; Guo, S.; Li, Z.; Liu, J.; McClain, J. D.; Sayfutyarova, E. R.; Sharma, S.; et al. PySCF: The Python-based simulations of chemistry framework. *Wiley Interdiscip. Rev. Comput. Mol. Sci.* **2018**, *8* (1), e1340.

(66) Sun, Q.; Zhang, X.; Banerjee, S.; Bao, P.; Barbry, M.; Blunt, N. S.; Bogdanov, N. A.; Booth, G. H.; Chen, J.; Cui, Z.-H.; et al. Recent developments in the PySCF program package. *J. Chem. Phys.* **2020**, *153* (2), 024109.
(67) Valiev, M.; Bylaska, E. J.; Govind, N.; Kowalski, K.; Straatsma, T. P.; Van Dam, H. J. J.; Wang, D.; Nieplocha, J.; Apra, E.; Windus, T. L.; et al. NWChem: A comprehensive and scalable open-source solution for large scale molecular simulations. *Comput. Phys. Commun.* **2010**, *181* (9), 1477-1489.
(68) Lu, T.; Chen, F. Multiwfn: A multifunctional wavefunction analyzer. *J. Comput. Chem.* **2012**, *33* (5), 580-592.
(69) Lehtola, S.; Steigemann, C.; Oliveira, M. J. T.; Marques, M. A. L. Recent developments in libxc — A comprehensive library of functionals for density functional theory. *SoftwareX* **2018**, *7*, 1-5.
(70) Becke, A. D. A multicenter numerical integration scheme for polyatomic molecules. *J. Chem. Phys.* **1988**, *88* (4), 2547-2553.
(71) Hirshfeld, F. L. Bonded-atom fragments for describing molecular charge densities. *Theor. Chim. Acta* **1977**, *44* (2), 129-138.
(72) Parr, R. G.; Ayers, P. W.; Nalewajski, R. F. What is an atom in a molecule? *J. Phys. Chem. A* **2005**, *109* (17), 3957-3959.
(73) Heidar-Zadeh, F.; Ayers, P. W.; Verstraelen, T.; Vinogradov, I.; Vöhringer-Martinez, E.; Bultinck, P. Information-theoretic approaches to atoms-in-molecules: Hirshfeld family of partitioning schemes. *J. Phys. Chem. A* **2018**, *122* (17), 4219-4245.
(74) Fievez, T.; Sablon, N.; De Proft, F.; Ayers, P. W.; Geerlings, P. Calculation of Fukui functions without differentiating to the number of electrons. 3. Local Fukui function and dual descriptor. *J. Chem. Theory Comput.* **2008**, *4* (7), 1065-1072.
(75) Pearson, R. G. *Chemical Hardness*; Weinheim: Wiley-VCH, 1997.
(76) Pearson, R. G. The principle of maximum hardness. *Acc. Chem. Res.* **1993**, *26* (5), 250-255.
(77) Gázquez, J. L.; Cedillo, A.; Vela, A. Electrodonating and electroaccepting powers. *J. Phys. Chem. A* **2007**, *111* (10), 1966-1970.
(78) Gázquez, J. L.; Franco-Pérez, M.; Ayers, P. W.; Vela, A. Temperature-dependent approach to chemical reactivity concepts in density functional theory. *Int. J. Quantum Chem.* **2019**, *119* (2), e25797.
(79) Perdew, J. P.; Zunger, A. Self-interaction correction to density-functional approximations for many-electron systems. *Phys. Rev. B* **1981**, *23* (10), 5048-5079.
(80) Hait, D.; Head-Gordon, M. Delocalization errors in density functional theory are essentially quadratic in fractional occupation number. *J. Phys. Chem. Lett.* **2018**, *9* (21), 6280-6288.
(81) Peach, M. J. G.; Teale, A. M.; Helgaker, T.; Tozer, D. J. Fractional electron loss in approximate DFT and Hartree–Fock theory. *J. Chem. Theory Comput.* **2015**, *11* (11), 5262-5268.
(82) Martin, J. M. L. Ab initio total atomization energies of small molecules — towards the basis set limit. *Chem. Phys. Lett.* **1996**, *259* (5), 669-678.
(83) Bultinck, P.; Cardenas, C.; Fuentealba, P.; Johnson, P. A.; Ayers, P. W. How to compute the Fukui matrix and function for systems with (quasi-)degenerate states. *J. Chem. Theory Comput.* **2014**, *10* (1), 202-210.
(84) Denbigh, K. G. The polarisabilities of bonds—I. *Trans. Faraday Soc.* **1940**, *36* (0), 936-948, 10.1039/TF9403600936.
(85) Clarys, T.; Stuyver, T.; De Proft, F.; Geerlings, P. Extending conceptual DFT to include additional variables: Oriented external electric field. *Phys. Chem. Chem. Phys.* **2021**, *23* (2), 990-1005, 10.1039/D0CP05277A.
(86) Ghanty, T. K.; Ghosh, S. K. Correlation between hardness, polarizability, and size of atoms, molecules, and clusters. *J. Phys. Chem.* **1993**, *97* (19), 4951-4953.
(87) Simón-Manso, Y.; Fuentealba, P. On the density functional relationship between static dipole polarizability and global softness. *J. Phys. Chem. A* **1998**, *102* (11), 2029-2032.

(88) Langenaeker, W.; Demel, K.; Geerlings, P. Quantum-chemical study of the Fukui function as a reactivity index: Part 2. Electrophilic substitution on mono-substituted benzenes. *Journal of Molecular Structure: THEOCHEM* **1991**, *234*, 329-342.
(89) Peng, D.; Yang, W. Fukui function and response function for nonlocal and fractional systems. *J. Chem. Phys.* **2013**, *138* (18), 184108.
(90) Yang, W.; Parr, R. G.; Pucci, R. Electron density, Kohn–Sham frontier orbitals, and Fukui functions. *J. Chem. Phys.* **1984**, *81* (6), 2862-2863.
(91) Morell, C.; Grand, A.; Gutiérrez-Oliva, S.; Toro-Labbé, A. Using the reactivity-selectivity descriptor Δf(r) in organic chemistry. In *Theoretical and Computational Chemistry*, Toro-Labbé, A. Ed.; Vol. 19; Elsevier, 2007; pp 101-117.
(92) Bader, R. F. W. Nearsightedness of electronic matter as seen by a physicist and a chemist. *J. Phys. Chem. A* **2008**, *112* (51), 13717-13728.
(93) Kitaura, K.; Morokuma, K. A new energy decomposition scheme for molecular interactions within the Hartree-Fock approximation. *Int. J. Quantum Chem.* **1976**, *10* (2), 325-340.
(94) Ziegler, T.; Rauk, A. A theoretical study of the ethylene-metal bond in complexes between copper(1+), silver(1+), gold(1+), platinum(0) or platinum(2+) and ethylene, based on the Hartree-Fock-Slater transition-state method. *Inorg. Chem.* **1979**, *18* (6), 1558-1565.
(95) Fernández, I.; Bickelhaupt, F. M. The activation strain model and molecular orbital theory: Understanding and designing chemical reactions. *Chem. Soc. Rev.* **2014**, *43* (14), 4953-4967, 10.1039/C4CS00055B.
(96) Khaliullin, R. Z.; Cobar, E. A.; Lochan, R. C.; Bell, A. T.; Head-Gordon, M. Unravelling the origin of intermolecular interactions using absolutely localized molecular orbitals. *J. Phys. Chem. A* **2007**, *111* (36), 8753-8765.
(97) Geerlings, P.; Van Alsenoy, C.; De Proft, F. The linear response function as a descriptor of non-covalent interaction: Hydrogen and halogen bonds. *Theor. Chem. Acc.*, accepted.
(98) Prigogine, I.; Defay, N. *Chemical Thermodynamics*; Longman, 1954, Chapter 1.

Table 1. List of CDFT quantities for di- and polyatomic systems where only the off-diagonal values are shown for the linear response function and the softness kernel (the values for ethane, ethene and ethylene pertain the two carbon atoms). In the Fukui functions the heavy and light atoms in a given molecule are denoted by subscript A and B respectively. Hardness η and hardness condition $\eta^{\pm}$ are obtained via **Eqn. 2 and 13,** respectively.

Label	μ^-	μ^+	η	η^-	η^+	S	χ_{AB}	s_{AB}^-	s_{AB}^+	f_A^-	f_A^+	f_B^-	f_B^+
LiH	-0.1601	-0.0578	0.0512	0.2875	-0.7193	19.5429	1.0502	3.4295	-1.4107	0.6441	1.0181	0.3559	-0.0181
LiBr	-0.2056	-0.0702	0.0677	0.3130	-0.7135	14.7744	0.9412	2.0357	-0.0812	0.7202	0.0621	0.2798	0.9379
LiCl	-0.2133	-0.0667	0.0733	0.3451	-1.1119	13.6359	0.8310	2.0255	-0.2739	0.7013	0.0427	0.2987	0.9573
LiF	-0.2216	-0.0569	0.0824	0.4632	-1.6678	12.1402	0.6391	2.2800	-0.6201	0.5978	0.0016	0.4022	0.9984
NaH	-0.1552	-0.0670	0.0441	0.2484	0.0499	22.6808	1.3961	3.1572	0.0041	0.7219	0.9339	0.2781	0.0661
NaBr	-0.1863	-0.0860	0.0501	0.3011	-0.0336	19.9551	1.2408	3.0858	0.2050	0.6822	0.0786	0.3178	0.9214
NaCl	-0.1901	-0.0836	0.0533	0.3299	-0.1029	18.7762	1.1074	3.1018	-0.2050	0.6607	0.0506	0.3393	0.9494
NaF	-0.1808	-0.0755	0.0526	0.4250	-0.1514	19.0031	0.8880	3.8517	-0.8809	0.4758	0.9996	0.5242	0.0004
CN^-	0.0319	0.2822	0.1252	0.3389	0.3090	7.9898	1.2227	0.6500	0.6355	0.3751	0.3680	0.6249	0.6320
N_2	-0.3708	-0.0611	0.1549	0.4126	0.4088	6.4576	1.0030	0.6114	0.6114	0.5000	0.5000	0.5000	0.5000
CO	-0.3280	-0.0668	0.1306	0.4076	0.3841	7.6565	0.9296	0.6562	0.7478	0.2929	0.3242	0.7071	0.6758
NO^+	-0.8501	-0.5319	0.1591	0.4909	0.4940	6.2865	0.8499	0.6526	0.6919	0.3952	0.4312	0.6048	0.5688
CO_2	-0.3290	-0.0042	0.1624	0.3869	0.3746	6.1583	0.5722	-0.0068	0.1687	0.3788	0.2984	0.2423	0.4032
SO_3	-0.2996	-0.1278	0.0859	0.3143	0.3067	11.6401	0.5561	0.0685	0.3168	0.2017	0.3418	0.2661	0.2194
HBr	-0.2727	-0.0440	0.1143	0.3562	0.2452	8.7460	0.6055	0.3422	1.5113	0.8764	0.5893	0.1236	0.4107
HCl	-0.2915	-0.0254	0.1331	0.4003	0.2268	7.5154	0.5275	0.3781	1.3487	0.8599	0.5188	0.1401	0.4812
HF	-0.3345	0.0065	0.1705	0.6008	0.0263	5.8661	0.3826	0.6353	0.8745	0.7766	0.3110	0.2234	0.6890
SiH_4	-0.3130	0.0118	0.1624	0.2930	0.2281	6.1575	0.3572	0.0058	0.0274	0.3810	0.5129	0.1547	0.1218
BF_3	-0.3644	-0.0101	0.1772	0.3478	0.2965	5.6449	0.3347	-0.0587	0.1345	0.2738	0.1584	0.1786	0.5249
H_2O	-0.2483	0.0085	0.1284	0.4772	0.1698	7.7876	0.3182	0.5980	0.4169	0.6212	0.2526	0.1894	0.3737
NH_3	-0.2148	0.0151	0.1149	0.4137	0.1635	8.7000	0.2567	0.4677	0.2026	0.5150	0.1973	0.1617	0.2676
CH_4	-0.3467	0.0308	0.1887	0.3732	0.1535	5.2991	0.2020	0.0767	0.0119	0.3009	0.2024	0.1748	0.1994
C_2H_2	-0.2624	-0.0029	0.1297	0.3573	0.3033	7.7087	0.8120	0.3455	0.1751	0.3875	0.3578	0.1125	0.1422
C_2H_4	-0.2473	-0.0317	0.1078	0.3162	0.2823	9.2792	0.5433	0.3038	0.1991	0.3021	0.2828	0.0989	0.1086
C_2H_6	-0.2987	0.0241	0.1614	0.3057	0.1562	6.1954	0.1829	-0.0643	-0.1055	0.1384	0.1118	0.1205	0.1294

Table 2. Total atomization energy $\sum D_e$ and hardness conditions $\eta^{\pm}$ for H_2O obtained by 19 common density functionals (with indication of their components) the first two being LDAs, the remaining ones GGAs.

DFAs	$\sum D_e$	η^-	η^+	exchange	correlation
SVWN5	0.4304	0.4782	0.1554	Slater	VWN5
SPW92	0.4301	0.4781	0.1553	Slater	PW92
BP86	0.3877	0.4755	0.1989	Becke88	P86
PW91	0.3799	0.4768	0.1044	PW91	PW91
BPW91	0.3741	0.4760	0.1945	Becke88	PW91
mPW91	0.3766	0.4762	0.1706	mPW91	PW91
PBE	0.3787	0.4772	0.1698	PBE	PBE
revPBE	0.3684	0.4765	0.1849	revPBE	PBE
RPBE	0.3669	0.4770	0.1619	RPBE	PBE
OPBE	0.3782	0.4778	0.1959	OPTX	PBE
HTBS	0.3748	0.4750	0.1682	HTBS	PBE
BLYP	0.3753	0.4771	0.2125	Becke88	LYP
OLYP	0.3795	0.4788	0.2206	OPTX	LYP
KT1	0.3804	0.4695	0.1576	KT1	KT1
KT2	0.3601	0.4711	0.1603	KT2	KT2
KT3	0.3620	0.4748	0.2001	KT3	KT3
HTCH407	0.3783	0.4805	0.0960	HTCH407	HTCH407
HTCH147	0.3789	0.4780	0.1584	HTCH147	HTCH147
HLE16	0.3828	0.4896	0.1656	HLE16	HLE16
Exp.[82]	0.3710				

Table 3. Condensed hardness kernel or hardness matrix $\eta_{AB}^{\pm}$ using hardness conditions and the normal modes of electron population of water. The eigenvalues h and the corresponding eigenvectors $\boldsymbol{U}$ corresponding to the population normal modes (PNM) are tabulated in descending order of the eigenvalue.

η_{AB}^{-}	O	H	H
O	0.7263	0.1075	0.1075
H	0.1075	2.0165	0.1504
H	0.1075	0.1504	2.0165
PNM	*1*	*2*	*3*
h	2.1825	1.8662	0.6870
$\boldsymbol{U_O}$	-0.1022	-0.0000	-0.9948
$\boldsymbol{U_H}$	-0.7034	0.7071	0.0722
$\boldsymbol{U_H}$	-0.7034	-0.7071	0.0722
η_{AB}^{+}	O	H	H
O	1.0474	-0.1268	-0.1268
H	-0.1268	1.2032	-0.6630
H	-0.1268	-0.6630	1.2032
PNM	*1*	*2*	*3*
h	1.8662	1.1044	0.4832
$\boldsymbol{U_O}$	0.0000	0.9530	0.3029
$\boldsymbol{U_H}$	-0.7071	-0.2142	0.6739
$\boldsymbol{U_H}$	0.7071	-0.2142	0.6739

Table 4. Total electronic energy and energy components from the functional expansion of conceptual DFT **Eqn. 30**. for di-atomic and 10-electron molecules selected from **Table 1**.

Name	E_{el}	E_{μ^-}	E_{μ^+}	E_{ρ}	E_{η^-}	E_{η^+}	E_{f^-}	E_{f^+}	E_{χ}
CH_4	-53.92	-3.47	0.31	-120.07	-18.66	-7.67	38.23	25.05	56.53
NH_3	-68.45	-2.15	0.15	-155.90	-20.69	-8.18	42.20	28.44	77.44
H_2O	-85.53	-2.48	0.08	-199.07	-23.86	-8.49	49.45	32.66	101.68
HF	-105.55	-3.34	0.06	-250.48	-30.04	-1.32	60.21	37.06	130.89
HCl	-467.64	-5.25	-0.46	-1109.21	-64.85	-36.74	134.32	105.19	318.75
HBr	-2587.41	-9.82	-1.58	-6178.68	-230.84	-158.89	476.93	393.26	1431.49
N_2	-133.21	-5.19	-0.86	-303.81	-40.44	-40.06	89.38	87.25	139.35
CO	-135.78	-4.59	-0.94	-311.07	-39.95	-37.64	83.06	81.60	146.83

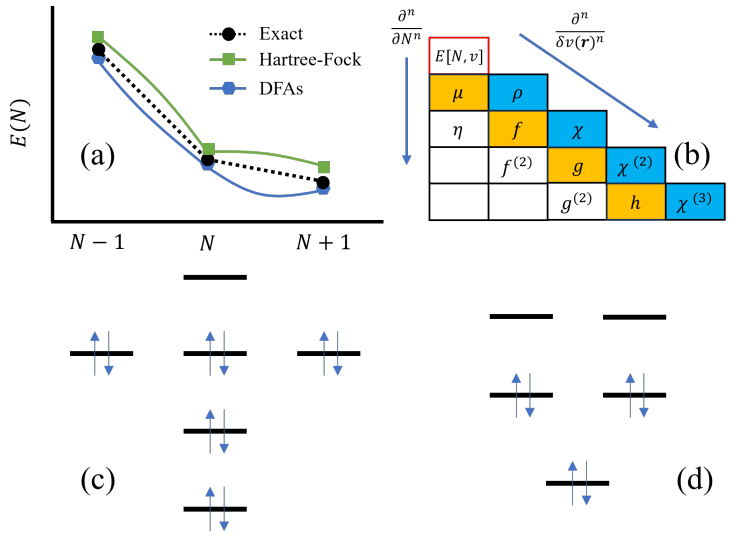

Scheme 1. (a) schematic E *vs* N curves for exact functional, most DFAs and Hartree-Fock method indicating piecewise-linear, -convex and -concave behavior respectively (b) analytical conceptual DFT "stairs" under 0K limit, blue and orange regions indicating zero and first order N-derivatives, and white blocks are second or higher order N-derivatives whose analytical evaluation is hampered by the derivative discontinuity problem leading the corresponding "conditions'' (see text) (c) molecular orbital diagram for methane and (d) π molecular orbital diagram for benzene.

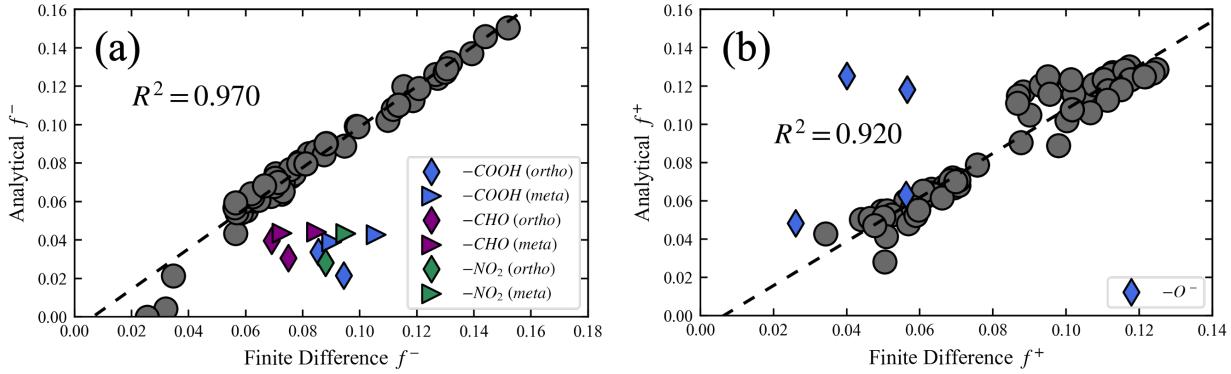

Figure 1. Linear correlation between Fukui function (a) f^- and (b) f^+ calculated by both analytical and finite difference approach for benzene with different substituents, outliners are highlighted (see text).

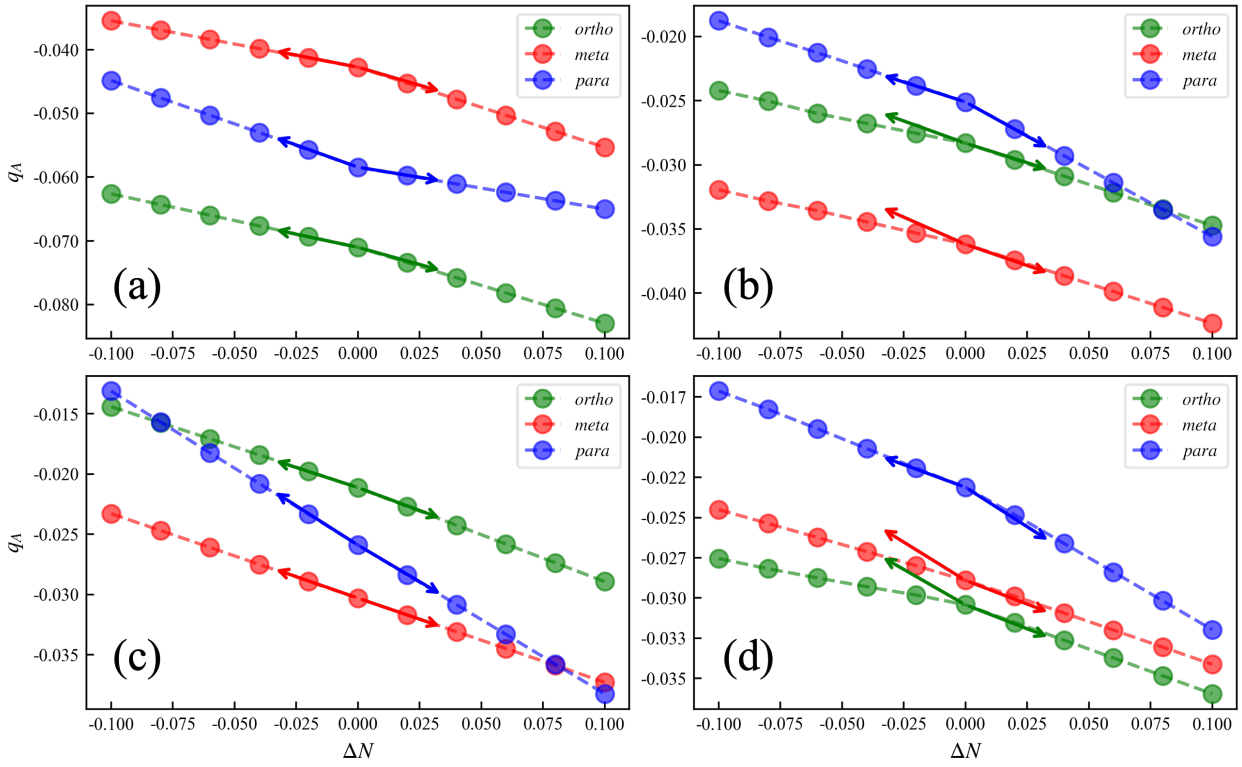

Figure 2. Behavior of Hirshfeld charge at ortho, meta and para position with small fractional occupation number (up to +/-0.01; dashed line) for substituted benzene systems: (a) -OH, (b) -CHO, (c) -CN and (d) -NO_2. The arrows point to the out-of-range cation and anion values calculated with integer occupation.

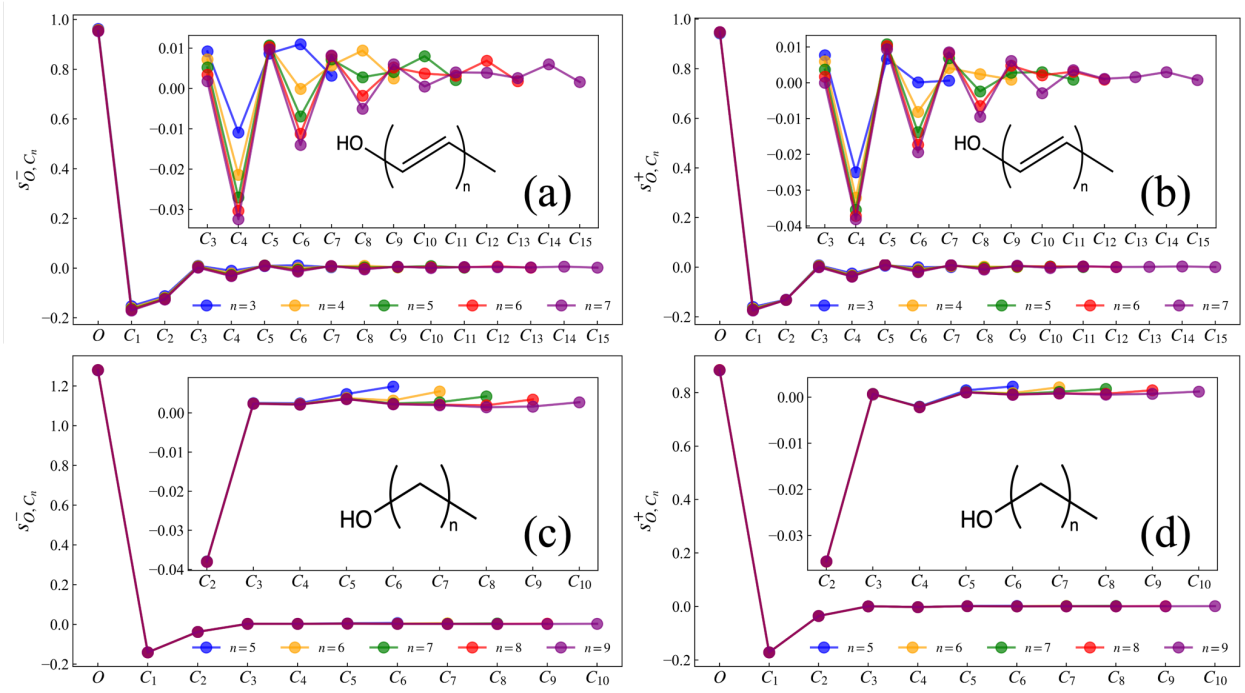

Figure 3. Condensed softness kernel values $s^{\pm}_{O,C_n}$ for 1-OH substituted poly-alkenes (a), (b) and linear alkane (c), (d) chains with the perturbation fixed at the oxygen atom.

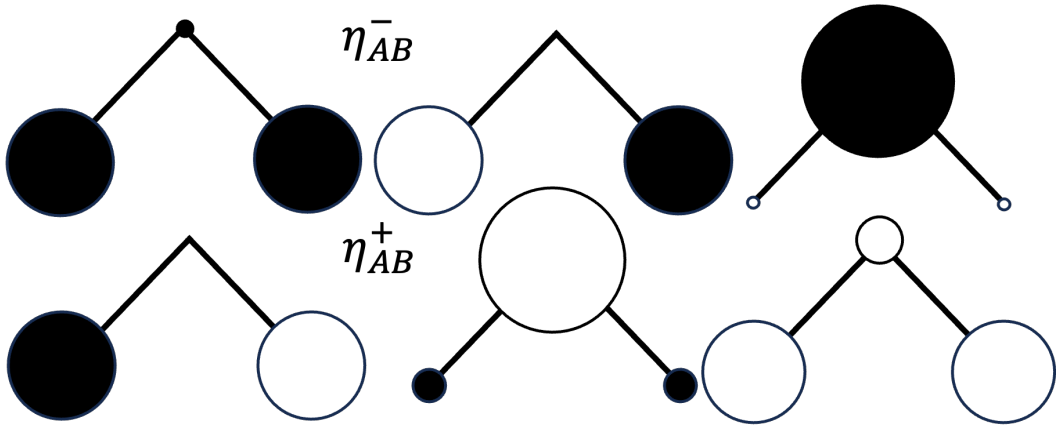

Figure 4. Nalewajski diagram of the normal modes of electron population displacements for water with the same sequence as in **Table 3**, where the inflow and outflow of electrons is represented by white and black circles respectively. The circle radius denotes the relative magnitude of these changes.

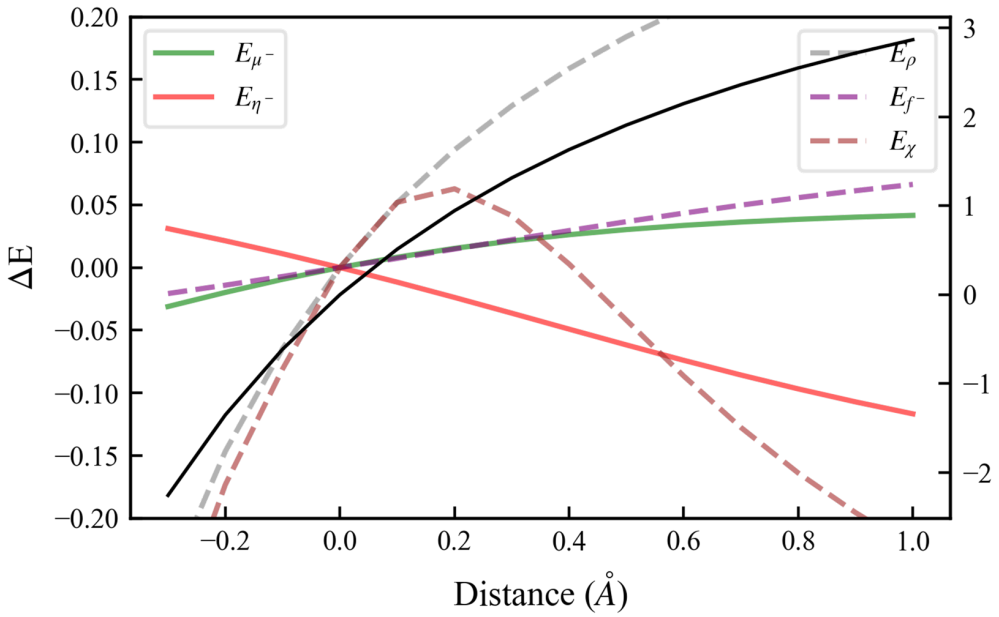

Figure 5. Changes of the energy (black) and its components for HF upon bond compression or stretching using the functional expansion of conceptual DFT **Eqn. 30**. Difference in distance w.r.t. equilibrium distance upon compression or elongation is given in abscissa (up to -0.3 and +1.0Å respectively). Left legend uses the energy scale at the left, analogously for the right legend/scale.

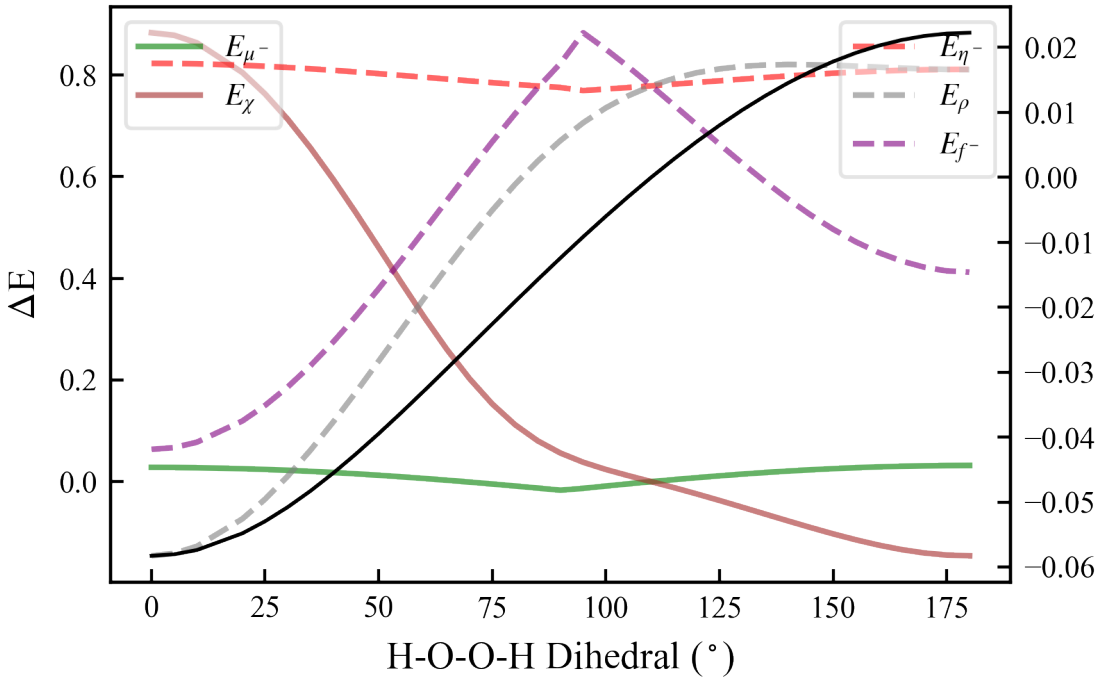

Figure 6. Changes of the energy (black) and its components during the H_2O_2 dihedral rotation process from 0 to 180 degree using the functional expansion of conceptual DFT **Eqn. 30**. Left legend uses the energy scale at the left, analogously for the right legend/scale.

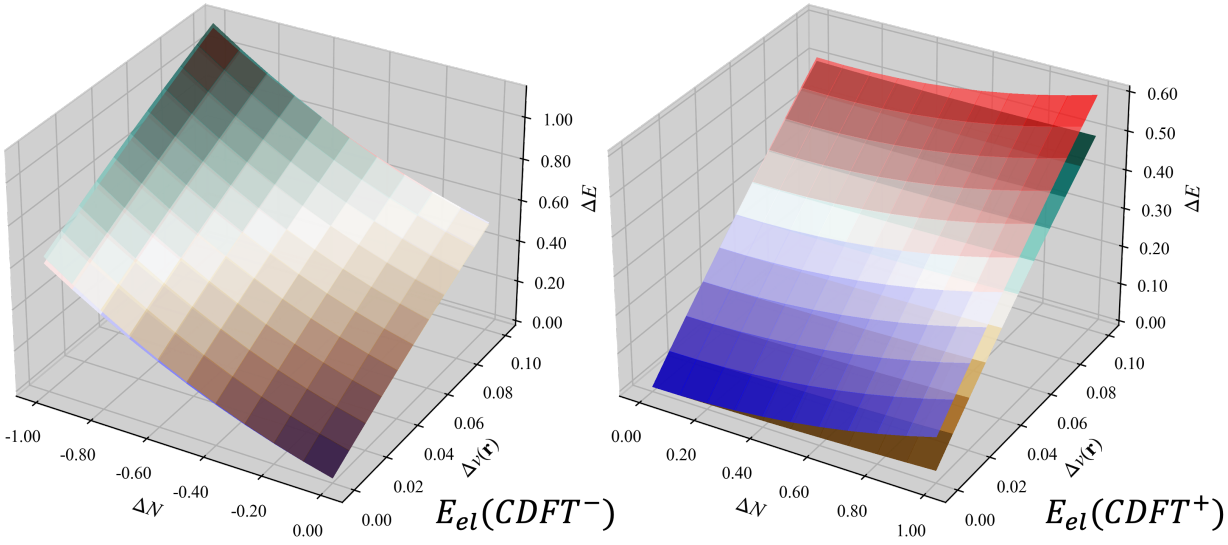

Figure 7. Electronic energy difference ΔE_{el} of hydrogen fluoride calculated from DFA (PBE/cc-pVTZ) (blue-white-red color code) compared to the second order Taylor expansion **Eqn. 28** (brown-white-green color code) with fractional occupation from -1 to 1 and bond stretching from equilibrium 0.0 to 0.1Å.

Graphical abstract